

1 **Penicillium chrysogenum** as a fungal factory for feruloyl esterases

2 Laura García-Calvo ^{1,2}; Raquel Rodríguez-Castro¹; Ricardo V. Ullán ^{1,3}; Silvia M. Albillos ⁴; Marta
3 Fernández-Aguado ¹; Cláudia M. Vicente ^{1,5}; Kristin F. Degnes ⁶; Håvard Sletta ⁶; Carlos Barreiro ⁷.

4

5 **Affiliations:**

6 ¹ INBIOTEC (Instituto de Biotecnología de León), Avda. Real 1 - Parque Científico de León, 24006
7 León, Spain.

8 ² Present Address: Department of Biotechnology and Food Science, NTNU Norwegian University of
9 Science and Technology, N-7491 Trondheim, Norway.

10 ³ Present Address: mAbxience, Upstream Production, Parque Tecnológico de León, Julia Morros, S/N,
11 Armunia, 24009 León, Spain.

12 ⁴ Área de Bioquímica Y Biología Molecular, Departamento de Biotecnología Y Ciencia de los
13 Alimentos, Facultad de Ciencias, Universidad de Burgos, 09001 Burgos, Spain.

14 ⁵ Present Address: TBI, Université de Toulouse, CNRS, INRAE, INSA, 31077 Toulouse, France.

15 ⁶ Department of Biotechnology and Nanomedicine, SINTEF Industry, Richard Birkelands Vei 3 B, 7034
16 Trondheim, Norway.

17 ⁷ Área de Bioquímica Y Biología Molecular, Departamento de Biología Molecular, Universidad de
18 León, Campus de Vegazana, 24007 León, Spain.

19 Corresponding authors: Ricardo V. Ullán rvicu@unileon.es and Carlos Barreiro c.barreiro@unileon.es

20 Laura García-Calvo and Raquel Rodríguez-Castro contributed equally to this work and should be
21 considered co-first authors.

22 **Abstract**

23 Plant biomass is a promising substrate for biorefinery, as well as a source of bioactive compounds,
24 platform chemicals, and precursors with multiple industrial applications. These applications depend on
25 the hydrolysis of its recalcitrant structure. However, the effective biological degradation of plant cell
26 walls requires several enzymatic groups acting synergistically, and novel enzymes are needed in order
27 to achieve profitable industrial hydrolysis processes. In the present work, a feruloyl esterase (FAE)
28 activity screening of *Penicillium* spp. strains revealed a promising candidate (*Penicillium rubens*
29 Wisconsin 54–1255; previously *Penicillium chrysogenum*), where two FAE-ORFs were identified and
30 subsequently overexpressed. Enzyme extracts were analyzed, confirming the presence of FAE activity
31 in the respective gene products (PrFaeA and PrFaeB). PrFaeB-enriched enzyme extracts were used to
32 determine the FAE activity optima (pH 5.0 and 50–55 °C) and perform proteome analysis by means of
33 MALDI-TOF/TOF mass spectrometry. The studies were completed with the determination of other
34 lignocellulolytic activities, an untargeted metabolite analysis, and upscaled FAE production in stirred

35 tank reactors. The findings described in this work present *P. rubens* as a promising lignocellulolytic
36 enzyme producer.

37

38 **Key Points**

- 39 • Two *Penicillium rubens* ORFs were first confirmed to have feruloyl esterase activity.
- 40 • Overexpression of the ORFs produced a novel *P. rubens* strain with improved activity.
- 41 • The first in-depth proteomic study of a *P. rubens* lignocellulolytic extract is shown.

42 **Keywords** : Fungi, *Penicillium rubens*, *Penicillium chrysogenum*, Lignocellulose, Feruloyl esterase,
43 Extracellular proteome

44

45 **Introduction**

46 Approximately 500–1000 million years ago, fungi diverged from a common ancestor with animals. This
47 event marked the beginning of evolutionary processes that have enabled fungi to colonize and thrive in
48 markedly different environments, becoming one of the major eukaryotic lineages (Muggia and Grube
49 2018; Stajich et al. 2009). Although some unicellular forms exist, fungi are typically characterized by a
50 filamentous vegetative form and absorptive, heterotrophic nutrition (McLaughlin et al. 2009). Fungi
51 play important roles in practically all known ecosystems. Their symbiotic relationships are pivotal in
52 the expansion and colonization of new habitats. Saprotrophic fungi are key players in nutrient cycles,
53 whereas pathogenic fungi affect other fungi, bacteria, plants, and animals, including human beings
54 (Lutzoni et al. 2004). Besides, fungi have a negative impact on human societies and economies, being
55 responsible for economic losses in fields such as health and agriculture (Bhatnagar et al. 2002; Cleveland
56 et al. 2003; De Lucca 2007; Mitchell et al. 2016; Wagacha and Muthomi 2008). Fortunately, their
57 positive impact is also noteworthy, since they are some of the most relevant producers of pharmaceutical
58 secondary metabolites such as antibiotics, only surpassed by Actinobacteria (Barreiro et al. 2012a). This
59 is an important trait, given the current threat to global health caused by microbial antibiotic resistance
60 (Barreiro and Barredo 2021). Moreover, fungi produce useful primary metabolites, such as organic acids
61 and fatty acids, and they have applications in the food industry (e.g., bread or fermented beverages)
62 (Ward 2012).

63 Due to their powerful enzymatic machinery, fungi are interesting hosts for the production of
64 heterologous and endogenous enzymes (Gifre et al. 2017; Mäkelä et al. 2014). The global industrial
65 enzyme market is constantly growing and obtained an estimated value of 8.2 billion USD in 2015
66 (Kumar et al. 2014; Manisha 2017). The website Marketresearch.com (<https://www.marketresearch.com/>) valued the global enzymes market in 2019 at 8.6 billion USD, and it could reach 14.5 billion USD
67 by 2027. Nowadays, more than 700 commercial products in over 40 industry sectors (e.g., agriculture,
68

69 food) are commercially available. Among them, applications in the food and beverage industries stand
70 out, reaching up to 2.0 billion USD in 2016 (Arnau et al. 2020; Chapman et al. 2018; Patel et al. 2016).
71 Particularly, fungal lignocellulolytic enzymes are capable of degrading lignocellulose, which is the main
72 component of dry plant biomass and the most abundant renewable organic resource on the planet (Jäger
73 and Büchs 2012). Around 140 billion tons of biomass are produced from the global agricultural sector
74 every year that are considered as a by-product or waste (Tripathi et al. 2019; Zuin and Ramin 2018).
75 The hydrolysis of lignocellulose releases fermentable sugars, platform chemicals, precursors,
76 biopolymers, and bioactive molecules with industrial applications (Guerriero et al. 2016). Among the
77 latter, hydroxycinnamic acids, such as caffeic, p-coumaric, sinapic, and ferulic acid, are of special
78 interest. Ferulic acid is a bioactive compound with multiple properties, namely, antiinflammatory,
79 antihepatotoxic, antioxidant (protecting the skin against UV-mediated oxidative damage),
80 anticarcinogenic, antimicrobial, antiviral, and antithrombotic. Besides, it can be used as a natural food
81 preservative and as a precursor in the production of industrially interesting substances, such as the
82 flavoring agent vanillin (Mathew and Abraham 2004). However, to release these compounds, plant cell
83 wall hydrolysis is required, a process that is complex due to the recalcitrance of this structure (Lynd
84 et al. 2002). To achieve this hydrolysis, physicochemical pretreatments (acid, alkali, hydrothermal,
85 oxidizing agents) and biological treatments (lignocellulolytic enzymes) are used. The bio-logical
86 treatments need milder reaction conditions, causing fewer side reactions, being safer, less energy
87 consuming, and environmentally friendlier (Pérez et al. 2002). Among lignocellulolytic enzymes,
88 feruloyl esterases (FAEs, EC 3.1.1.73) are a subclass of the carboxylic acid esterases (EC 3.1.1) that
89 cleave ester bonds between hydroxycinnamic acids and carbohydrates of the plant cell wall (Fazary and
90 Ju 2007). This rupture affects the stability of plant cell walls and, thus, assists in their deconstruction
91 (Faulds 2010). Taking into account recent studies on the prevalence of FAEs in fungal genomes, there
92 are still many fungal FAEs to be discovered and characterized (Dilokpimol et al. 2016). Considering the
93 multiple applications of FAEs in industries such as textile, pulp and paper, pharmaceutical, food, feed,
94 and biofuels (Fazary and Ju 2008), further research to find novel FAEs is needed.

95 *Penicillium rubens* (formerly, *Penicillium chrysogenum*) (Houbraken et al. 2011; Thom 1910) is a
96 fungal species belonging to phylum Ascomycota, subphylum *Pezizomycotina*, order *Eurotiales*.
97 *Penicillium* species are widely distributed in nature, occurring in soils, decaying vegetable matter,
98 animal skin, food products, etc. (Houbraken et al. 2011). They act as decomposers of organic materials
99 and can synthesize a wide range of secondary metabolites, including mycotoxins and antibiotics, such
100 as penicillin, produced by *P. rubens* (Fierro et al. 2022; Visagie et al. 2014). Given the economic and
101 social significance of these secondary metabolites, different omics analyses have been applied to unravel
102 the metabolic machinery of *P. rubens* (García-Estrada et al. 2020). The full genome of one of the
103 classical antibiotic-producing strains (*P. rubens* Wisconsin 54–1255) has been published (van den Berg
104 et al. 2008) as well as studies on transcriptomes (Terfehr et al. 2017; van den Berg et al. 2008),
105 intracellular, extracellular, and microbody proteomes (Domínguez-Santos et al. 2017; Jami et al. 2010a,

106 b, 2018; Kiel et al. 2009). Their strong degradative enzymatic machinery has made it a suitable genus
107 for the screening of novel lignocellulolytic enzymes, such as xylanases, cellulases, or feruloyl esterases
108 (Castanares et al. 1992; Chávez et al. 2006; Donaghy et al. 1998; Kroon et al. 2000; Phuengmaung et al.
109 2019; Terrasan et al. 2016).

110 The present work aimed to discover, overexpress, and characterize novel FAEs with industrial
111 applications, produced by *P. rubens* strains. Moreover, proteomic techniques and metabolite analyses
112 were carried out to study the extracellular proteome of this fungus when cultured under FAE production
113 conditions, using the lignocellulosic substrate sugar beet pulp (SBP) as a carbon source and inducer of
114 the production of lignocellulolytic enzymes.

115 **Materials and methods**

116 **Substrates and reagents**

117 Ferulic acid, p-coumaric acid, xylan from birchwood, 3,5-dinitrosalicylic acid (DNS), ethyl 4-hydroxy-
118 3-methoxy-cinnamate (ethyl ferulate, EF), 4-nitrophenol, 4-nitro-phenyl β -D-glucopyranoside (pNPG),
119 4-nitrophenyl β -D-cellobioside (pNPC), 4-nitrophenyl β -D-xylopyranoside (pNPX), D-(+)-gluconic
120 acid δ -lactone, and carboxymethylcellulose sodium salt (CMC) were purchased from Sigma-Aldrich
121 (Burlington, MA, USA). Methyl 4-hydroxy-3-methoxy-cinnamate (methyl ferulate, MFA) was acquired
122 from Alfa Aesar (Haverhill, MA, USA).

123 The natural lignocellulosic substrate processed milling oat fiber powder (OAT) was purchased from a
124 local provider. SBP as pellets was kindly provided by Sociedad Cooperativa General Agropecuaria
125 ACOR (Valladolid, Spain). Pellets were ground before use, obtaining thick dust with a diameter of
126 particles of 1–5 mm.

127 **Strains and cultivation**

128 *Escherichia coli* DH5 α (Hanahan 1983) was grown in Luria–Bertani medium (Miller 1972)
129 supplemented with 100 μ g/mL of ampicillin and employed for plasmid maintenance and propagation.

130 Five penicillin-producing fungal strains were used: *P. rubens* NRRL 1951, *P. rubens* Wisconsin 54–
131 1255 (ATCC 28089), *P. rubens* AS-P-78, *P. rubens* AS-P-99, and *Penicillium notatum* NRRL-1249.
132 Sporulation of mycelia was achieved by growth on Power medium (Casqueiro et al. 1999) at 28 °C for
133 5 days. To initiate seed cultures, spores were scraped, inoculated in 500-mL non-baffled flasks
134 containing 100-mL PMMY defined medium adjusted to pH 6.0 (Jami et al. 2010a) and grown at 28 °C,
135 250 rpm for 24 h (seed culture). Submerged cultures were initiated after inoculating 10% (v/v) seed
136 culture in 500-mL non-baffled flasks with 100 mL of SBP medium (M-SBP; 2.0-g/L NH_4NO_3 ; 1.0-g/L
137 K_2HPO_4 ; 0.5-g/L $\text{MgSO}_4 \cdot 7\text{H}_2\text{O}$; 0.5-g/L KCl; 1.0-g/L soy peptone; 1.0-g/L D-glucose; 18.7-mg/L
138 FeSO_4 , pH 5.0; 20-g/L SBP) or oat medium (M-OAT; same composition as M-SBP, but 20 g/L OAT,
139 instead of SBP). Cultures were incubated at 28 °C, 250 rpm, for up to 1 week. Three independent
140 biological replicates were used per strain. Bioreactor cultivations of the fungal strains were carried out

141 on M-SBP medium at 28 °C and 0.8 vvm (vessel volume per minute) air flow rate, using 10% (v/v) of
142 submerged cultures in PMMY medium grown for 24 h as the seed culture. The shaking rate was adjusted
143 so the dissolved oxygen values remained above 60% throughout the cultivation. pH, sterile air flow rate,
144 dissolved oxygen, shaking rate, and temperature were monitored.

145 **Molecular biology techniques**

146 **gDNA extraction and Southern blotting**

147 Genomic DNA (gDNA) from *P. rubens* Wisconsin 54–1255 was extracted from mycelium grown for
148 24 h, at 25 °C and 250 rpm, in PMMY medium, following the protocol described by Casqueiro and co-
149 workers (Casqueiro et al. 1999). gDNA samples were digested with the endonucleases *Hind*III and *Apa*I
150 (New England Biolabs) and separated using 0.7% (w/v) agarose gel electrophoresis. Gels were
151 subsequently blotted onto nitrocellulose uncharged Hybond-N membranes (Amersham, GE Healthcare
152 Biosciences) and UV-fixed. Membranes were hybridized with specific DNA-based digoxigenin-labeled
153 probes, corresponding to the *faeA* and *faeB* gene sequences labeled using the DIG-High Prime kit
154 (Roche). For detection, membranes were incubated with alkaline phosphatase and an appropriate
155 substrate (CDP-Star; Roche). Hybridization chemiluminescent signals were recorded on X-ray films and
156 developed employing Kodak chemicals.

157 **Plasmid design and construction**

158 Plasmids **pSfaeA** and **pSfaeB** were constructed to overexpress PrFaeA and PrFaeB, respectively, in
159 *P. rubens* Wisconsin 54–1255. The *faeA* gene was amplified from *P. rubens* Wisconsin 54–1255 gDNA,
160 using Phusion High-Fidelity DNA Polymerase (New England Biolabs) and oligonucleotides *faeA*-F and
161 *faeA*-R (Table 1). For the *faeB* gene, *faeB*-F, and *faeB*-R oligonucleotides were used (Table 1). These
162 primers include the *Bgl*III and *Stu*I restriction sites. The PCR products (933 bp for *faeA* and 1643 bp for
163 *faeB*) were cloned in the *Bgl*III-*Stu*I site of plasmid pIBRC43BglIII (Kosalková et al. 2009), controlled
164 by the strong *Aspergillus awamori* *gdh* gene promoter and ended by the *Saccharomyces cerevisiae* *cycl*
165 transcriptional terminator, generating plasmids pSfaeA and pSfaeB, respectively.

166 **Cloning and expression**

167 *P. rubens* protoplasts were transformed according to a method described previously (Ullán et al. 2007).
168 The parent strain *P. rubens* Wisconsin 54–1255 was cotransformed with either pSfaeA or pSfaeB, plus
169 plasmid pJL43 (Gutiérrez et al. 1991), the latter carrying a phleomycin resistance cassette. Selection
170 was carried out in a solid Czapek minimal medium supplemented with sorbitol (1 M) as an osmotic
171 stabilizer and phleomycin (35 µg/mL) as the selection agent.

172 **Quantitative PCR (RT-qPCR)**

173 Total RNA was extracted from the parent strain *P. rubens* Wisconsin 54–1255 and the two transformants
174 B13 and A78, at 24, 48, and 72 h of cultivation in M-SBP medium, with the RNeasy Mini Kit (Qiagen).

175 Total RNA was treated with RQ1 RNase-Free DNase (Promega) and RNase-free DNase (Qiagen),
176 following the manufacturer's protocols. Complementary DNA (cDNA) was obtained using the
177 SuperScript III One-Step RT-PCR with Platinum *Taq* DNA polymerase (Invitrogen), with 2.5 µg of
178 DNase-treated RNA as a template. Amplifications were carried out using 20-µL SYBR Premix Ex Taq
179 (TaKaRa), according to the following program: 10 min at 95 °C, 40 cycles of 15 s at 95 °C and 34 s at
180 62 °C. Two biological replicates and three technical replicates were used. Oligonucleotides (Table 1)
181 were designed to produce PCR products close to the mRNA 5' end, by means of the Primer3 software
182 (Rozen and Skaletsky 2000). Green fluorescence from SYBR was normalized with the passive reference
183 dye ROX (carboxy-X-rhodamine). The resulting data were processed according to the Pfaffl method
184 (Pfaffl 2001), normalizing the results using the constitutive *actA* gene as a reference. Amplification
185 efficiency (E) was calculated using triplicates of six standard 1:5 serial dilutions of gDNA. E value was
186 determined by the equation $E = -1 + 10(-1/\text{slope})$ (Rasmussen 2001), with a coefficient of correlation
187 $R^2 > 0,99$.

188 **FAE activity screening**

189 FAE activity was evaluated following the method described by Donaghy and McKay (Donaghy and
190 McKay 1994) modified as follows. Selected fungal strains were grown on Power medium plates for 5
191 days at 28 °C, until sporulation. Triplicate plugs (10-mm diameter) from these plates were inserted in
192 Petri dishes containing a 1% (w/v) Bacto agar (BD) sterile solution (50 °C) supplemented with 1.5-mL
193 of filtered EF diluted in ethanol (0.05 g/mL ethanol). EF plates containing the fungal plugs were
194 incubated for 12 days at 28 °C. Controls were set up on Bacto agar plates without EF. After incubation,
195 plates were stained with a 0.04% (w/v) bromocresol green solution, for 15 min, and washed twice for 5
196 min using NaCl 0.9% (w/v). FAE activity was identified as a yellow halo against a blue background,
197 due to the pH decrease produced by the release of ferulic acid.

198 **Protein recovery from cultures**

199 Secreted protein samples were obtained from cultivation broths recovered by filtration through Nyal
200 45-µm pore membranes. The flow-through was centrifuged twice at $3,220 \times g$, 30 min at 4 °C, and the
201 remaining pellet (fungal biomass) was dried at 80 °C, for 7 days, to determine dry weight. The resulting
202 supernatant was cleared using 0.22-µm pore Stericup™ filtering devices (Millipore®). Soluble protein
203 in the filtrate was recovered by precipitation with ammonium sulfate at 100% saturation at 4 °C,
204 according to the EnCorBio ammonium sulfate calculator (Wingfield 1998). The ammonium sulfate
205 saturated solution was stirred gently for at least 12 h. After precipitation, proteins were pelleted by
206 centrifugation at $10,400 \times g$, 4 °C, 1 h. Pellets were dried for 5 min and resuspended in acetate buffer
207 0.02 N pH 5.0 [100-fold concentration (v/v)]. These soluble protein samples are the “enzyme extracts”
208 employed in the proteomic techniques, activity assays, and enzyme kinetics. All steps were performed
209 on ice or in a cold room at 4 °C, to minimize proteolysis.

210 **Quantitative FAE activity assays**

211 FAE activity was assessed quantitatively by HPLC–UV, measuring the release of ferulic acid after
212 hydrolysis of the synthetic substrate MFA, and 10 μ L of enzyme extract was added to 190 μ L of a 0.05%
213 (w/v) MFA solution in acetate buffer 0.1 N pH 5.0. Reactions were performed at a standard temperature
214 (37 °C) for 20 min and terminated by boiling for 5 min. Samples were recovered by centrifugation at
215 16,168 \times g for 5 min and filtered through 0.22- μ m syringe filters (Fisherbrand). The released
216 hydroxycinnamic acids were measured using a Mediterranean Sea C18 reversed phase column (4.6 \times
217 150 mm, 3 μ m, Teknokroma) thermostated to 20 °C, according to previously described HPLC methods
218 (García-Calvo et al. 2018). Quantitation was performed by interpolating from linear standard curves.
219 FAE activity was expressed in units (U), defined as the amount of enzyme required to release 1 μ mol of
220 product per min under the tested conditions. All measurements were run in triplicates and controls were
221 set up using acetate buffer 0.1 N pH 5.0 instead of enzyme extract.

222 **Determination of optimal FAE activity conditions**

223 Reactions were set by adapting the protocol described in the section above (“Quantitative FAE activity
224 assays”). To determine the pH optimum, reactions were run at the standard temperature of 37 °C, using
225 citrate–phosphate 0.1 M pH 3.0–7.0 instead of acetate buffer 0.1 N pH 5.0.

226 Temperature optimum was evaluated by means of FAE activity reactions performed in acetate buffer
227 0.1 N pH 5.0, at temperatures ranging from 37 to 60 °C. All reactions were run in triplicates for 20 min
228 and stopped by boiling for 5 min.

229 **FAE activity against natural substrates**

230 FAE activity against natural lignocellulosic substrates was determined through reactions performed at
231 175 rpm, 50 °C, for 1–5 h, employing 2% (w/v) SBP in acetate buffer 0.1 N pH 5.0 as a substrate.
232 Reactions were terminated by boiling for 5 min and filtered through 0.22- μ m syringe filters, before
233 measuring the release of ferulic acid by means of HPLC. FAE activity was expressed as microgram (μ g)
234 of ferulic acid released per milliliter (mL) of the reaction mixture.

235 **Cellulose and xylan degrading activity assays**

236 To determine cellulase activity, the three main enzymatic activities included in this group were analyzed:
237 endoglucanase (EC 3.2.1.4), exoglucanase (cellobiohydrolase; EC 3.2.1.91), and β -glucosidase (EC
238 3.2.1.21). The ability of *P. rubens* B13 enzyme extracts to efficiently degrade xylan was evaluated
239 through the determination of two of the main enzymatic groups involved: endoxylanase (EC 3.2.1.8)
240 and β -xylosidase (EC 3.2.1.37) (Chávez et al. 2006).

241 To analyze β -glucosidase, cellobiohydrolase, and β -xylosidase activities, an assay based on the release
242 of 4-nitrophenol after the hydrolysis of synthetic substrates was used (Li et al. 2016; Terrasan et al.
243 2016). Specific activities were expressed in units (amount of enzyme required to release 1 μ mol of 4-
244 nitrophenol per min under the tested conditions) per mg of total protein in the enzyme extract. Reactions
245 were set using 10- μ L enzyme extract in a final volume of 550 μ L substrate solution, incubated at 50 °C

246 and stopped by the addition of 550 μL 2% (w/v) Na_2CO_3 . Substrate solutions were (i) for β -glucosidase,
247 4-mM pNPG; (ii) for cellobiohydrolase, 4-mM pNPC supplemented with 1-mg/mL D-glucono-1,5- δ -
248 lactone; (iii) for β -xylosidase, 5-mM pNPX. All substrates were diluted in acetate buffer 0.1 N pH 5.0.
249 The sample's absorbance was measured at 405 nm, and the release of 4-nitrophenol was determined by
250 interpolating from a linear standard curve, prepared in triplicates under the same conditions.

251 *Endoglucanase* and *xylanase* activities were analyzed by means of the DNS assay for reducing sugars
252 (Ghose 1987; Mattéotti et al. 2012; Xiao et al. 2005). Reactions were performed by adding 10 μL
253 enzyme extract in a final volume of 500 μL substrate solution. Substrates were carboxymethylcellulose
254 (CMC) for endoglucanase and xylan from birchwood for xylanase, diluted 1% (w/v) in acetate buffer
255 0.1 N pH 5.0. Reactions were performed at 50 $^\circ\text{C}$ and terminated by the addition of 500 μL of DNS
256 reagent [1.4% DNS, 0.28% phenol, 0.07% sodium sulfite, 28% Na–K-tartrate (Rochelle salt), and 1.4%
257 NaOH]. Reactions were boiled for 5 min to develop the color, which was stabilized by cooling down
258 the tubes in an ice-water bath, for 5 min. The amount of released reducing sugars was calculated through
259 the absorbance of a linear standard curve at 540 nm for glucose (endoglucanase)/ xylose (xylanase)
260 prepared in triplicates under the same conditions. Specific endoglucanase/xylanase activity was
261 expressed in units per gram of total protein in the enzyme extract.

262 **Saccharification assays**

263 Enzyme extracts were added to a 2% (w/v) SBP solution in acetate buffer 0.1 N pH 5.0. Saccharification
264 reactions were run for 24 h at 50 $^\circ\text{C}$ and 175 rpm. Samples were boiled for 5 min and filtered through
265 0.22- μm syringe filters prior to HPLC analysis. The released mono and disaccharides (sucrose, glucose,
266 fructose, arabinose, and galactose) were determined by means of HPLC–UV (Waters), using an 8- μm
267 Transgenomic CARBOSEP COREGEL 87P column (300 \times 7,8 mm) thermostated to 90 $^\circ\text{C}$ and
268 following an isocratic method described elsewhere (García-Calvo et al. 2018).

269 **Enzyme extract treatment for proteomic analyses**

270 Enzyme extracts were recovered as detailed in the “Protein recovery from cultures” Material and
271 Methods section and treated prior to proteomic analyses. Proteins were precipitated at – 20 $^\circ\text{C}$,
272 overnight, by addition of an equal volume of prechilled 20% (w/v) TCA/acetone with 0.14% (w/v) DTT
273 (Jami et al. 2010b). Proteins were recovered by centrifugation at 3,220 \times g, 10 min, 4 $^\circ\text{C}$, and washed
274 twice with prechilled 0.07% (w/v) DTT in acetone and once with 80% (v/v) acetone/distilled water. The
275 precipitate was dried briefly and resuspended in sample buffer [8 M urea, 2% (w/v) CHAPS, 0.5% (v/v)
276 IPG buffer 3–11 NL (GE Healthcare), 100- mM DTT, and 0.002% bromophenol blue], gently shaken at
277 25 $^\circ\text{C}$, for 1 h. Soluble protein extracts were quantified through the Bradford assay (Bradford 1976) and
278 used immediately or frozen in aliquots at – 80 $^\circ\text{C}$.

279 **DIGE análisis**

280 Difference gel electrophoresis (DIGE) was performed according to the protocol described by Martínez-
281 Gomariz and co-workers (Martínez-Gomariz et al. 2009; Vasco- Cárdenas et al. 2013), with
282 modifications. Soluble protein extracts were cleaned from interfering substances using the 2D Clean-
283 Up Kit (GE Healthcare). Proteins were resuspended in 8 M urea, 4% (w/v) CHAPS, and 30 -mM Tris
284 pH 8.5. Protein labeling was performed on ice and in the dark, with 400 pmol/μL Cy dyes (Cy2, Cy3,
285 Cy5) per 50 μg of protein replicate. Labeling reactions were terminated by adding 10 mM lysine, for 10
286 min. Samples corresponding to one single gel were combined, and the final volume was completed to
287 350 μL with rehydration buffer [8 M urea, 60 mM DTT, 2% (w/v) CHAPS, 0.5% IPG buffer, pH 3–11
288 (GE Healthcare), 0.01% bromophenol blue]. Immobiline® Drystrip pH 3–10 NL 18-cm strips (GE
289 Healthcare) were used for isoelectric focusing (IEF), according to the following protocol, at 20 °C: 1 h,
290 0 V, and 12 h, 30 V (rehydration); 2 h, 60 V; 1 h, 500 V; 1 h, 1000 V; 30 min gradient, to 8000 V; up to
291 7 h at 8000 V until 50 kVh. Focused IPG gels went through two equilibration steps prior to the second
292 dimension: (i) 15 min equilibration in a buffer containing 6-M urea, 50 mM Tris–HCl (pH 8.8),
293 30%(v/v) glycerol, 2% (w/v) SDS, 0.002% bromophenol blue, and 1% (w/v) DTT; (ii) 15 min
294 equilibration in the same buffer, substituting DTT for 4.0% (w/v) iodoacetamide. Equilibrated IPG gels
295 were subjected to the second dimension in 12.5% polyacrylamide SDS-PAGE in an Ettan Dalt Six
296 apparatus (GE Healthcare), at 25 °C, according to the following program: 45 min, 3 W/ gel; 3.5–4 h, 18
297 W/gel. Precision Plus Protein Standards (Bio-Rad) were employed as molecular weight markers.

298 Gels were imaged by means of an Ettan™ DIGE Imager (GE Healthcare) with CyDye filters and 100
299 μm pixel size. Image analysis was performed using the DeCyder™ differential analysis software v7.0
300 (GE Healthcare) and the Differential In-gel Analysis (DIA) module. The Biological Variance Analysis
301 (BVA) module was used. For comparison, the internal standard image gel with the greatest number of
302 spots was chosen as a master gel. The statistical analyses between groups included the determination of
303 the average ratio, unpaired Student's *t* test, and ANOVA. FDR (false discovery rate) was applied to
304 reduce false positives. To be considered as differentially expressed with statistical significance, protein
305 spots needed to comply with three conditions: (i) be present in at least 70% of gel images; (ii) show at
306 least a 1.5-fold average volume ratio, and (iii) have *p* values lower than 0.05.

307 **Analysis of proteins in the enzyme extracts**

308 To analyze and identify the proteins present in the *P. rubens* Wisconsin 54–1255 B13 enzyme extracts,
309 two-dimensional gel electrophoresis was carried out (Jami et al. 2010a). Three gels corresponding to
310 three biological replicates from independent cultures were analyzed; 400 μg of soluble proteins
311 resuspended in sample buffer was subjected to IEF on an IPGphor apparatus, by means of 4–7 NL
312 Immobiline™ 18-cm IPG strips (GE Healthcare). IEF and, subsequently, the second dimension were
313 performed as described previously (“DIGE analysis” Material and Methods section). After 2-DE, gels
314 were stained following the “blue silver” colloidal Coomassie staining method (Candiano et al. 2004;
315 Jami et al. 2010a). Gels were scanned by means of an ImageScanner III (GE Healthcare), calibrated

316 using a grayscale marker (Eastman Kodak Co.), and the Labscan 5.00 (v1.0.8) software (GE Healthcare).
317 Gel analysis was carried out with the ImageMaster™ 2D Platinum v 5.0 software (GE Healthcare).
318 Automatic spot detection was verified manually to avoid artifacts (background noise, bubbles, streaks,
319 etc.). To quantify and compare spots, spot normalization was carried out based on relative volumes,
320 defined as the volume of each spot divided by the total volume of all the spots in the gel. Protein spots
321 were matched using landmark features. Protein spots present in the three replicates were considered for
322 identification.

323 **Protein identification**

324 Selected protein spots were manually excised from stained gels, enzymatically digested with trypsin
325 (Havliš et al. 2003), and processed as detailed in previous works (Jami et al. 2010a). To analyze samples,
326 a 4800 Proteomics Analyzer (MALDI-TOF/TOF, AB Sciex) was employed, using a 4700 Proteomics
327 analyzer calibration mixture (Cal Mix 5, AB Sciex) as external calibration. Additionally, MS spectra
328 were internally calibrated considering peptides from the trypsin autodigestion. MALDI-TOF/TOF
329 analysis using the 4000 Series Explorer v3.5.3 software (AB Sciex) originated peptide mass fingerprints
330 (PMF). Up to 65 peptides from one spot were gathered and represented as monoisotopic molecular
331 weights with a signal-to-noise ratio (S/N) greater than 20. Known contaminant ions, such as peptides
332 derived from trypsin and keratin digestion, were not considered for later MS/MS analyses. The 6 most
333 intense precursors with $S/N > 20$ from each MS spectrum were selected for MS/MS analysis with CID,
334 using atmospheric gas, in 2-kV ion reflector mode and with a mass window of ± 7 Da. Mascot generic
335 files combining MS (PMF) and tandem MS (MS/MS) spectra were created automatically. For protein
336 identification, Mascot generic files were employed to query a nonredundant protein database using a
337 local license of Mascot v2.2 (Matrix Science) through the Global Protein Server v3.6 (Applied
338 Biosystems). The following search parameters set for peptide mass fingerprints and tandem MS spectra
339 were established: (i) taxonomy, all entries (date 2018.10.23; 8,745,091 sequences, 3,903,651,808
340 residues); (ii) fixed and variable modifications were considered, Cys as S-carbamidomethyl derivative
341 and Met as oxidized methionine; (iii) one missed cleavage site was tolerated; (iv) precursor tolerance
342 was 50 ppm and MS/MS fragment tolerance was 0.3 Da; (v) peptide charge was set to 1 + ; (vi) the
343 employed enzyme was trypsin.

344 Protein identifications achieved by the abovementioned method were only considered acceptable if the
345 global Mascot score was greater than 83, with a significance level of $p < 0.05$. The global Mascot score
346 uses probability-based scoring and indicates the probability that the observed match is a random event.
347 A higher Mascot score corresponds to a lower probability of a random match (Perkins et al. 1999).

348 **Metabolite analyses**

349 Metabolite extraction was performed from 96 h M-SBP and M-OAT cultures, grown as detailed in the
350 “Strains and cultivation” Material and Methods section. Triplicate samples of supernatant, DMSO, and
351 methanol extracts from independent cultivations were extracted as follows: 5 mL of broth were

352 centrifuged twice at $3,220 \times g$, for 30 min, and the supernatant and pellet were separated. The supernatant
353 was filtered through 0.22- μm syringe filters (Millipore), and the mycelium pellets were resuspended in
354 10-mL methanol or 10-mL dimethyl sulfoxide (DMSO) by vortexing for 30 s and extracted for 45 min
355 in a rotating mixer at room temperature. Enzyme extracts were prepared as described in the “Protein
356 recovery from cultures” Material and Methods section. The extracts were analyzed by LC-DAD-QTOF-
357 MS with MS1 and MS2 following a previously described method with modifications (Degnes et al.
358 2017).

359 A Zorbax bonus RP column (2.1×50 mm, $3.5 \mu\text{m}$) was employed to separate metabolites, with formic
360 acid and acetonitrile as the mobile phase at a 0.3 mL/min flow. LC-DAD isoplots were generated with
361 Python. Centroid LC-MS data were processed with the MassHunter Qualitative Analysis Software v.
362 B.04.00 (Agilent Technologies) and Mass Profiler Professional software v2.1.5 (MPP; Agilent
363 Technologies). A search for known compounds was performed against databases such as METLIN PCD
364 (Agilent Technologies) and a PubChem database for bioactive compounds.

365 **Results**

366 **Selection of endogenous FAE-producing strains**

367 The first goal of this work was to select a *Penicillium* spp. strain with endogenous FAE (feruloyl
368 esterase) activity, in order to find putative FAEs and subsequently overexpress them through genetic
369 engineering. This species was chosen based on its high evolutionary proximity with species of the genus
370 *Aspergillus* (van den Berg et al. 2008), known as one of the most interesting fungal enzyme producers,
371 whose FAEs have been thoroughly studied (Dilokpimol et al. 2016, 2017; Koseki et al. 1998, 2009b;
372 Mäkelä et al. 2018; Zhang et al. 2013).

373 Two wild-type *Penicillium* spp. strains (*P. notatum* NRRL-1249 and *P. rubens* NRRL-1951) and three
374 industrial strains used in antibiotic production, well adapted to grow under industrial conditions (*P.*
375 *rubens* Wisconsin 54-1255, AS-P-78 and AS-P-99), were analyzed by means of a FAE activity plate
376 assay (Supplementary Fig. S1). The EF (ethyl ferulate) hydrolysis efficiency of each strain was
377 expressed through the enzymatic index [EI = (diameter of the colony + diameter of the degradation halo)
378 / diameter of the colony] (Braga et al. 2014).

379 *P. notatum* NRRL-1249, *P. rubens* NRRL-1951, and *P. rubens* Wisconsin 54-1255 displayed higher
380 FAE activity than *P. rubens* AS-P-78 and AS-P-99 (Fig. 1A). The two most promising *P. rubens* strains
381 were further compared by means of the release of ferulic acid from SBP (sugar beet pulp) after
382 submerged culture on M-SBP medium at 28 °C, 250 rpm, for 120 h (Fig. 1B). The results showed a
383 similar capacity to release ferulic acid from SBP in submerged culture. Given this similar activity, *P.*
384 *rubens* Wisconsin 54-1255 was selected for the enhancement of its FAE production, due to the existence
385 of optimized genetic modification techniques, its suitability for growth and sporulation in a laboratory
386 environment, and the availability of its sequenced genome (van den Berg et al. 2008).

387 **Establishment of optimal growth conditions and FAE activity reaction conditions**

388 The impact of change in cultivation conditions on FAE production was evaluated. Furthermore, the
389 conditions for the FAE activity assay were optimized to select the optimal conditions for further
390 experiments. SBP was used as a carbon source in these cultivations and as a natural inducer of FAEs
391 (Benoit et al. 2006; de Vries et al. 2002; Sakamoto et al. 2005) and MFA (methyl ferulate) as a synthetic
392 substrate for FAE activity reactions (Ralet et al. 1994; Record et al. 2003; Wang et al. 2016a).

393 **Agitation**

394 Both agitated and static culture conditions have previously been used to produce FAEs (Fazary and Ju
395 2007; Gopalan et al. 2015; Kumar et al. 2011; Topakas et al. 2007). To compare FAE production in both
396 states, *P. rubens* Wisconsin 54–1255 was grown in M-SBP liquid medium at 28 °C with (250 rpm) and
397 without agitation (Fig. 2A). FAE activity was determined through the amount of ferulic acid released
398 from the substrate SBP, measured from filtered culture supernatants by means of HPLC. Cultivations
399 shaken at 250 rpm showed higher FAE activity, particularly at the last sampling time (96 h).

400 **Seed culture**

401 Two types of seed cultures were tested: (i) a spore suspension obtained from Power medium plates
402 grown for 5 days at 28 °C and inoculated directly into cultivation flasks with M-SBP medium (spores
403 from one Power medium plate per 100 mL of M-SBP medium); (ii) 10% (v/v) of a seed culture grown
404 from spores in plates, on PMMY medium, at 28 °C and 250 rpm for 24 h. Cultivation broth samples
405 were recovered from cultures grown on M-SBP medium for 96 h, subsequently filtered, and precipitated
406 using ammonium sulfate to obtain enzyme extracts according to the “Protein recovery from cultures”
407 Material and Methods section. FAE activity was quantitatively determined through the release of ferulic
408 acid after the hydrolysis of the synthetic substrate MFA, analyzed by HPLC. The results showed that
409 slightly higher FAE activity was obtained when using 10% (v/v) of a submerged culture grown for 24 h
410 on PMMY medium as seed culture (Fig. 2B).

411 **pH and temperature optima**

412 To determine the optimal FAE activity conditions of the enzyme extract recovered from *P. rubens*
413 Wisconsin 54–1255 grown on M-SBP, FAE reactions against MFA were carried out at a standard
414 temperature of 37 °C and pH ranging from 3.0 to 7.0. FAE activity was detected from pH 3.0 to 6.0
415 (Fig. 3A) with a pH optimum at pH 5.0. The temperature optimum was analyzed at the optimal pH (pH
416 5.0) and temperatures from 37 to 60 °C. The enzyme extract had high activity over a wide temperature
417 range, with an optimum in the range of 45–55 °C (Fig. 3B); 50 °C was thus selected as the optimal
418 temperature for further experiments, as higher temperatures lead to greater variation, with consistently
419 reduced FAE enzymatic activity above 55 °C.

420 **Optimal enzyme dosage and reaction time for the hydrolysis of SBP**

421 The optimal amount of enzyme extract and reaction time for the release of ferulic acid from the natural
422 substrate SBP were evaluated as described in the “FAE activity against natural substrates” Material and
423 Methods section. Tests were carried out using several enzymatic doses (0, 0.1, 0.5, 1.5, and 2.1 mg of
424 enzyme extract per g of SBP) and at two different reaction times (1 and 5 h). The results showed that
425 the maximal absolute ferulic acid release was achieved when adding 1.5 mg of enzyme extract per g of
426 SBP, with 5-h incubation (Fig. 4). Furthermore, the release of ferulic acid per unit of time was greater
427 with a shorter reaction time (1-h incubation, instead of 5 h).

428 **Cloning and overexpression of feruloyl esterases from *P. rubens* Wisconsin 54–1255 in the natural** 429 **host**

430 **Genome search for FAE-encoding genes**

431 Putative FAE encoding genes from *P. rubens* Wisconsin 54–1255 were identified by means of a
432 homology search with known FAE encoding genes from *Aspergillus* spp. (AnFaeA and AnFaeB
433 encoding genes), using the BLAST tool (Boratyn et al. 2013).

434 Two possible ORFs in *P. rubens* Wisconsin 54–1255 encoding putative enzymes with FAE activity
435 (ORFs Pc20g07010 and Pc12g08300) were identified. Both sequences have a pentapeptide with
436 conserved consensus sequence GX SXG, whose residue of serine belongs to the catalytic triad Ser-His-
437 Asp, characteristic of the serine protease and esterase families, also identified in *A. niger* AnFaeA
438 (Hermoso et al. 2004). These proteins were named PrFaeA and PrFaeB and their respective genes: *faeA*
439 and *faeB*, following the nomenclature proposed by Faulds and co-workers (Crepin et al. 2004; Faulds
440 2010; Faulds et al. 2003).

441 Apart from the previously mentioned ORFs, other putative FAE encoding genes present in *P. rubens*
442 Wisconsin 54–1255 genome have been reported in previous works, such as ORFs Pc13g15360,
443 Pc20g11110, and Pc21g17360 (Dilokpimol et al. 2016). However, in the present work, ORFs
444 Pc20g07010 and Pc12g08300 were selected for overexpression, as they showed the highest identity
445 percentages with AnFaeA (99% sequence coverage, 75% identity) and AnFaeB (100% sequence
446 coverage, 51% identity), respectively.

447 **Cloning and expression**

448 The PrFaeA and PrFaeB encoding sequences were cloned, separately, into the overexpression plasmid
449 pIBRC43BglIII (Kosalková et al. 2009), obtaining plasmids p*SfaeA* and p*SfaeB*, respectively. Two lines
450 of FAE overexpressing transformants were generated: (i) line A (overexpressing gene *faeA*) and (ii) line
451 B (overexpressing gene *faeB*).

452 More than 100 transformants were obtained from each line, 48 of which were randomly selected and
453 analyzed by means of FAE activity plate assays, as detailed in the “FAE activity screening” Material
454 and Methods section (Supplementary Fig. S2). The 8 transformants from line A and 10 from line B with
455 the highest FAE activity (higher EI and less deviation between replicas) were selected (line A: 1, 18,

456 31, 68, 71, 76, 78, and 84; line B: 1, 7, 10, 13, 17, 20, 27, 77, 83, and 88). Southern blotting verification
457 of selected transformants Southern hybridization was carried out with the selected transformants in order
458 to confirm the presence of the overexpression cassette (Supplementary Fig. S3). The results showed that
459 all transformants kept the endogenous respective FAE gene and that only some had incorporated the
460 integrative overexpression cassette (A68, A76, A78, B1, B7, B10, B13, B20, B77, B83). The complete
461 integration of the overexpression cassette was verified by means of DNA sequencing, using the primers
462 detailed in Table 1.

463 Three transformants of each line with the integrated overexpression cassette (A68, A76, A78, B13, B77,
464 and B83) were selected to perform quantitative FAE activity assays on both natural (SBP) and synthetic
465 substrates (MFA), at pH 5.0 and 50 °C (Fig. 5). Transformant A78 from line A and transformant B13
466 from line B stood out. B13 showed 14 times higher FAE activity than *P. rubens* Wisconsin-541255
467 against SBP and 90 times higher when MFA was used as a substrate. Transformants A78 and B13 were
468 chosen for further experiments.

469 **Gene expression analyses**

470 Gene expression of the *P. rubens* Wisconsin 54–1255 strain and transformants A78 and B13 was then
471 analyzed by RT-qPCR to verify that the increase in FAE activity was the result of an increase in the
472 expression of the *faeA* and *faeB* genes in the two overexpressed lines (Supplementary Figs. S4 and S5).
473 This assay showed that the *faeA* or *faeB* expression was increased in both transformants (A78 and B13,
474 respectively), obtaining the maximum expression at 24 h of incubation. Particularly noteworthy was the
475 B13 transformant, in which the expression of *faeB* at 24 h was 214 times higher than in the *P. rubens*
476 Wisconsin 54–1255 strain.

477 The A78 transformant was remarkably less active against the natural lignocellulolytic substrate SBP
478 than the B13 transformant. Given that SBP was the inducing substrate of choice in the present work,
479 B13 was chosen for further experiments. Previous studies have indicated that FAEs belonging to
480 category A according to the functional classification proposed by Crepin and co-workers have low or
481 no activity against SBP, whereas type B FAEs (such as PrFaeB) are the most active (Crepin et al. 2004;
482 Dilokpimol et al. 2016; Kühnel et al. 2012). Moreover, type A FAEs are induced by monocotyledonous
483 plants, such as corn or wheat, and not by dicotyledonous plants, such as sugar beet (Fazary and Ju 2007;
484 Zwane et al. 2014).

485 ***P. rubens* extracellular proteome analysis**

486 The differences in the extracellular proteome between *P. rubens* Wisconsin 54–1255 and the B13
487 transformant were evaluated through 2D-DIGE electrophoresis, using four biological replicates per
488 strain. Protein samples were obtained by ammonium sulfate precipitation of broths recovered at 72 h
489 cultivation in M-SBP medium, in Braun Biostat® B 20 L fermentors. As detailed in the “DIGE analysis”
490 Material and Methods section, protein spots that presented a 1.5-fold or greater variation between both

491 strains ($p < 0.05$) were selected for identification. 10 showed significant differences and 4 were
492 identified by means of trypsin digestion and MS analyses (MALDI-TOF/TOF). Two of them
493 corresponded to PrFaeB (Pc12g08300), which was the overexpressed FAE in the B13 transformant. The
494 fold change (ratio) of these protein spots was 4.49 and 4.78, indicating a higher PrFaeB production in
495 the overexpressed transformant *P. rubens* B13 (Supplementary Fig. S6).

496 Besides comparing the differences in the extracellular proteins secreted by *P. rubens* Wisconsin 54–
497 1255 and the B13 transformant, the complete extracellular proteome of the B13 transformant grown on
498 SBP was analyzed by means of 2D electrophoresis and MALDI-TOF/TOF MS protein identification.
499 As most proteins in the 2D-DIGE analyses were detected below pH 7.0, Immobiline® Drystrip pH 4–7
500 NL 18-cm strips were used for this experiment. Cultivation broths from 3 biological replicates were
501 recovered from 72-h M-SBP cultures in Braun Biostat® C 20 L bioreactors and precipitated with
502 ammonium sulfate. The secreted protein extract 2D reference map was obtained (Fig. 6), with 205
503 protein spots common to all three replicates. Out of the detected protein spots, 120 were successfully
504 identified by peptide mass fingerprinting and tandem MS (Table 2, Supplementary File S7). From them,
505 124 protein identifications were obtained; 102 identifications corresponded to several protein species
506 (isoforms) of 22 proteins, while the remaining 22 were unique protein species.

507 The SignalP 5.0 server was used to identify the presence of putative signal peptides in the identified
508 proteins (Almagro Armenteros et al. 2019; Nielsen 2017; Nielsen et al. 1997). Out of the total 124
509 protein species, 117 (94.35%) were predicted to have a signal peptide. Of the seven remaining proteins,
510 two protein species (1.61%) were predicted to present nonclassical secretion, according to the
511 SecretomeP 1.0 server (Bendtsen et al. 2004), and 5 did not present any of the mentioned signals. The
512 fact that most of the identified proteins presented putative signal peptides or nonclassical secretion
513 indicates low presence of intracellular proteins in the analyzed samples, and, thus, supports the absence
514 of important cell lysis processes at the selected sampling time.

515 Subsequently, functional annotation of the proteins identified in the enzyme extract was performed by
516 using the COG (clusters of orthologous groups of proteins) system, which includes eukaryote organisms
517 (KOG), via the eggNOG 5.0 online orthology resource (Fig. 7) (Huerta-Cepas et al. 2019; Tatusov et al.
518 2003). The main findings in these groups are summarized below.

519 **Plant cell wall degradation (proteins in COG G)**

520 The biological processes leading to plant cell wall degradation require different enzymatic groups that
521 act synergistically (de Souza 2013; Wei et al. 2009). As shown in Fig. 7, the majority of the identified
522 proteins were related to carbohydrate metabolism and transport (a total of 88 isoforms of 28 different
523 proteins). One of the most represented enzymatic groups was the cellulases, with 4 β -glucosidases (EC
524 3.2.1.21), which were identified from 5 protein spots; 2 exoglucanases (cellobiohydrolases, EC
525 3.2.1.91), identified from 8 spots; and an endoglucanase (endocellulase, 3.2.1.4), identified from 1 spot.

526 The synergistic action of these enzymatic groups is required to achieve the complete hydrolysis of
527 cellulose (Dashtban et al. 2009; Escamilla-Alvarado et al. 2017; Lynd et al. 2002).

528 One of the spots with higher relative volume (% volume, Supplementary File S7) in the reference map
529 (spot 113), with 3 isoforms present (spots 111, 112, and 113), was identified as a putative pectate lyase
530 (EC 4.2.2.2). Several other hemicellulases and pectinases were identified, including (i) α -L-
531 arabinofuranosidases (EC 3.2.1.55), (ii) endo-1,4-betaxylanase (EC 3.2.1.8), (iii) rhamnogalacturonan
532 endolyases (EC 4.2.2.23), (iv) exo-arabinanases, and (v) feruloyl esterases (EC 3.1.1.73). The strong
533 presence of matrix polysaccharide degrading enzymes may be due to the carbohydrate composition of
534 the lignocellulosic substrate which was used (SBP), as detailed in the Discussion section.

535 **Proteins related to the fungal cell wall (proteins in COGs G and M)**

536 In this category, 10 different proteins with 48 isoforms were identified from the analyzed partial
537 extracellular proteome. One of these distinct proteins was a β -N-acetylhexosaminidase (EC 3.2.1.52)
538 identified from the protein spot with the highest relative volume (spot 62; protein name Pc20g10360;
539 Supplementary File S7), as well as 16 more spots (a total of 17 isoforms). Moreover, 5 isoforms of
540 another putative β -N-acetylhexosaminidase (Pc22g24800), 2 and 3 isoforms of two chitinases
541 (Pc13g09520 and EN45_103640, respectively), and 3 isoforms of 2 endo- 1,3(4)- β -glucanases
542 (Pc16g08980 and Pc13g08730) were also identified. These enzymes are involved in the hydrolysis and
543 reorganization of chitin, one of the major components of most fungal cell walls (Díez et al. 2005; Zhao
544 et al. 2014), and its promoter has been patented for genetic engineering uses by Antibióticos León S.A.
545 (patent number WO/1998/039459) (Barredo Fuente et al. 1998).

546 **General cell metabolism (proteins in COGs E, O, C, M)**

547 The extracellular proteome analysis permitted the identification of 5 distinct putative proteases and
548 peptidases (protein names Pc22g15910, Pc13g09680, Pc21g14160, Pc20g09400, and Pc22g13950).
549 Other identified proteins belonging to this functional category were a glutaminase (Pc20g02640), an
550 amidase (Pc22g01750), 2 FAD-linked oxidoreductases (Pc21g12590, Pc18g05530), and a thioredoxin
551 reductase (Pc22g22810).

552 **Cell rescue, defense, and virulence (proteins in COGs C, P, Q)**

553 An important factor in the microbial ability to degrade plant cell walls is the capacity to tolerate or
554 remove toxic compounds derived from such degradation. In this regard, 10 isoforms of a single putative
555 catalase (Pc16g11860) were identified. Catalases catalyze the hydrolysis of hydrogen peroxide, which
556 can be produced as a consequence of the hydrolysis of plant cell walls, to H₂O and oxygen (Jami et al.
557 2010b). Catalases are also related to pathogenicity in fungal plant pathogens (Garre et al. 1998).

558 **Unknown function (proteins in COG S)**

559 Lastly, 13 isoforms of 4 different proteins whose biological function remains to be elucidated were
560 identified.

561 **Industrial applicability of *P. rubens* B13 enzyme cocktail**

562 The enzyme extract recovered from cultivations of *P. rubens* B13 grown on M-SBP showed promising
563 levels of FAE activity (14 times higher than the parent strain *P. rubens* Wisconsin 54–1255 against SBP,
564 and 90 times higher against MFA). To evaluate a possible industrial application, several studies were
565 conducted, including the determination of other lignocellulolytic activities acting synergistically, the
566 analysis of the saccharification capacity, and its suitability to be adapted to fermentation in a bioreactor
567 at higher culture volumes. Moreover, an untargeted metabolite study was performed to assess the
568 putative presence of bioactive metabolites in the enzyme extracts.

569 **Lignocellulolytic activities in the enzyme extract**

570 Commonly, commercial preparations for the hydrolysis of plant biomass include a mixture of
571 lignocellulolytic enzymes, instead of one single purified enzyme (Fazary and Ju 2008; Mäkelä et al.
572 2014). Considering this fact and the presence of a wide array of lignocellulolytic enzymes in the partial
573 extracellular proteome studied in this work, two of the most important group of activities were
574 determined: cellulase and xylanolytic activities. Reactions were performed with *P. rubens* B13 enzyme
575 extracts at pH 5.0 and 50 °C, to characterize the synergistic activities occurring simultaneously at the
576 optimal FAE activity conditions.

577 As shown in Table 3, *P. rubens* B13 enzyme extract presented all the five cellulase and xylanolytic
578 tested activities. This finding is in accordance with the identification of β -glucosidases, exoglucanases,
579 and β -xylosidases in *P. rubens* B13 extracellular proteome (“Plant cell wall degradation (proteins in
580 COG G)” Results section). Previous works have evaluated the cellulolytic and hemicellulolytic potential
581 of *Penicillium* spp. Song and co-workers determined these enzymatic activities in the hypercellulolytic
582 mutant *P. oxalicum* JU-A10, whose β -glucosidase values were over 4.5 times lower than those of *P.*
583 *rubens* B13 (Song et al. 2016). Moreover, when compared to *P. oxalicum* JU-A10, *P. rubens* B13
584 showed more than twice as high cellobiohydrolase activity and slightly higher β -xylosidase activity,
585 which points to *P. rubens* B13 as a promising strain to produce cellulolytic and hemicellulolytic
586 preparations.

587 The β -glucosidase, cellobiohydrolase, β -xylosidase, and endoxylanase activities in *P. rubens* B13
588 enzyme extracts were higher than in an enzyme cocktail obtained from *Alternaria alternata* PDA1,
589 which, in turn, showed higher endoglucanase values (García-Calvo et al. 2018). As the
590 cellobiohydrolase activity in the *A. alternata* PDA1 enzyme cocktail was remarkably lower than in the
591 *P. rubens* B13 enzyme extract (around 50 times lower), a combination of both preparations might be
592 able to enhance the degradation of plant biomass.

593 **Sugar beet pulp saccharification**

594 The industrial applications of fungal enzyme extracts such as the one obtained from *P. rubens* B13 are
595 related to their ability to hydrolyze plant cell walls and release simple sugars, a process which is known
596 as saccharification (Jimenez- Flores et al. 2010; Menon and Rao 2012; Micard et al. 1996; Ravalason et
597 al. 2012). The saccharification capacity of the enzyme extracts recovered from *P. rubens* Wisconsin 54–
598 1255 and transformant B13 was measured through the release of simple sugars determined by HPLC–
599 UV, after enzymatic reactions performed on SBP. Reactions were carried out for 24 h at pH 5.0, 50°C,
600 and 175 rpm, adding 15 mg of enzyme extract per gram of SBP. As shown in Table 4, the analyzed
601 extracts efficiently released limited quantities of arabinose, fructose, and glucose, none of which were
602 found in the control reactions without enzyme extracts. Besides, sucrose, which was found in the control
603 reactions, was not detected in the reactions employing enzyme extracts, which suggests the presence of
604 hydrolases that are capable of degrading the aforementioned disaccharide, such as invertases (Nuero and
605 Reyes 2002; Poonawalla et al. 1965).

606 **Scale-up of the PrFaeB production process**

607 In order to achieve production levels that are compatible with commercial uses, it is necessary to scale
608 up the fermentation process. The suitability of *P. rubens* B13 to cultivation in a bioreactor was assessed
609 by means of 5-L and 20-L cultivations in Braun Biostat® B and C fermentors, with working volumes
610 of 3 L and 12 L, respectively, as described in the “Strains and cultivation” Material and Methods section.
611 Two conditions were analyzed regarding cultivation pH: (i) uncontrolled pH (starting at pH 5.0) and (ii)
612 pH 5.0, controlled by the automatic addition of NaOH 1 M and HCl 1 N. Samples were recovered every
613 24 h to measure total protein, cell growth (dry weight), and FAE activity against the synthetic substrate
614 MFA.

615 According to the monitored cultivation parameters and the FAE activity values (Supplementary Figs.
616 S8.A and S8.B), cultivations carried out at pH 5.0 controlled automatically were preferable to achieve
617 higher FAE activity in the enzyme extracts. Besides, considering the monitored parameters and FAE
618 activity values, the optimal sampling time for the recovery of enzyme extracts was 24 h, in 5-L
619 fermentors (Supplementary Fig. S8C). In 20-L fermentors, FAE activity was slightly higher at 48 h;
620 however, this limited increase would not justify a 24-h extension of the cultivations, considering the
621 associated expenses and the delay in the recovery of the commercial products (Supplementary Fig. S9B).
622 These reasons indicated that the optimal cultivation time of *P. rubens* B13 in 20-L bioreactors for FAE
623 activity would also be 24 h.

624 The suitability of *P. rubens* B13 for cultivation in bioreactors (Supplementary Figs. S8.A and S9.A) as
625 well as the earlier sampling time for optimal FAE activity observed when grown in fermentors (24 h as
626 opposed to 96 h in flask cultivation) confirms this strain as a propitious FAE producer for industrial
627 applications.

628 **Metabolite analyses**

629 Enzymes are generally considered safe for industrial uses, as indicated by the lack of adverse effects in
630 oral toxicity and genotoxicity safety studies (Sewalt et al. 2016). However, as *P. rubens* is a well-known
631 antibiotic producer and is also capable of synthesizing other bioactive molecules, such as mycotoxins
632 (Fernández-Aguado et al. 2014; García-Estrada et al. 2011; Jami et al. 2010b), an untargeted metabolite
633 analysis was performed to study the presence of putative undesirable or hazardous compounds.

634 Supernatants, DMSO, and methanol extracts of pellets, as well as enzyme extracts prepared from *P.*
635 *rubens* B13 cultures on M-SBP and M-OAT media, were analyzed using three independent biological
636 replicates per condition. LC-DAD isoplots were generated to give an overview of which UV-absorbing
637 compounds were present in the different extracts (Supplementary File S10.A). For the MS data, only
638 those metabolites present in at least two of the three replicates of each condition were considered for
639 identification. A total of 88 masses were putatively annotated against METLIN PCD and a PubChem
640 database for bioactive compounds. Out of the 88 metabolites, 30 were present in both M-SBP and M-
641 OAT media, 29 were exclusive to M-SBP and 29 were only found in M-OAT. The putatively annotated
642 metabolites included peptides; fatty acids and related compounds; sphingolipids; glycerophospholipids;
643 vitamin D and related compounds; vitamin E and related compounds; sterols and related compounds, a
644 mycotoxin; antibiotics; and other bioactive metabolites (Supplementary File S10.B). Among the
645 detected metabolites were two categories that could affect the industrial applicability of the enzyme
646 extracts: a mycotoxin (aflatoxin B1) and two antibiotics (penicillin G and penicillin V). The possible
647 presence of penicillin was assessed by MS/MS fragmentation followed by comparison against the
648 METLIN database and the molecular networking database GNPS (Wang et al. 2016b). This approach
649 identified three masses with no database annotation, which were apparently related to penicillin G.

650 **Discussion**

651 The cleavage of the bonds that stabilize the plant cell wall, necessary for its deconstruction, is not a
652 trivial process, and it requires an assortment of lignocellulolytic enzymes that act synergistically
653 (Guerriero et al. 2016; Wei et al. 2009). Among these enzymatic groups, auxiliary enzymes, such as
654 FAEs, have been the subject of an increasing number of studies in the last decades (Fazary and Ju 2007;
655 Udatha et al. 2012). The discovery of novel FAEs with different optimal activity conditions is needed
656 to achieve more effective industrial processes in fields such as biofuels, paper, food, and feed industries
657 (Dilokpimol et al. 2016; Gopalan et al. 2015; Topakas et al. 2007). Moreover, FAEs catalyze the release
658 of hydroxycinnamic acids, which are a key component in lignocellulose recalcitrance to hydrolysis and
659 have several commercial applications, as antioxidants and precursors for the synthesis of valuable
660 compounds like vanillin (Alam et al. 2016; de Oliveira et al. 2015; Mathew and Abraham 2006; Ou and
661 Kwok 2004; Taofiq et al. 2017). As heterotrophic osmotrophs, fungi are natural producers of
662 extracellular hydrolases, including carbohydrate-active enzymes (CAZymes). In this regard, the present
663 work aimed to identify and overexpress novel fungal FAEs with potential industrial applications.

664 *P. notatum* NRRL-1249, *P. rubens* NRRL-1951, and *P. rubens* Wisconsin 54–1255 showed higher FAE
665 activity than *P. rubens* AS-P-78 and AS-P-99 (Fig. 1A). The two strains with the highest FAE activity
666 in the plate assay were the least genetically modified: *P. notatum* NRRL-1249 and *P. rubens* NRRL-
667 1951. These results indicate that strain selection for antibiotic production has negatively impacted their
668 endogenous FAE activity, presumably as a consequence of major modifications in primary and
669 secondary metabolism (Barreiro et al. 2012b; Jami et al. 2010a, 2010b). Two ORFs found in the *P.*
670 *rubens* Wisconsin 54–1255 genome encoding possible enzymes with FAE activity (Pc20g07010 and
671 Pc12g08300) were functionally annotated according to their homology with previously described fungal
672 FAEs (Dilokpimol et al. 2016; Udata et al. 2011). The observed results prove for the first time that the
673 overexpression of the aforementioned ORFs led to an increase in the release of ferulic acid from
674 synthetic FAE substrates such as EF and MFA, which indicates that the respective encoded proteins
675 effectively show FAE activity.

676 The PrFaeA sequence comprised 5 conserved domains related to lipase activity (cd00519, pfam01764,
677 PLN02802, PLN03037 and COG3675), and the most recent FAE phylogenetic classification assigned
678 it to subfamily 7, which includes FAEs that are related to lipases (Dilokpimol et al. 2016). On the other
679 hand, the PrFaeB sequence included one single conserved domain (pfam07519) related to tannases and
680 was included in subfamily 1. FAEs seem to have evolved from diverse enzymatic groups and present
681 differences in their sequences and structural features, which can explain their distinct specificity and
682 activity toward various substrates.

683 The extracellular proteome reference map from *P. rubens* Wisconsin 54–1255 has been studied in
684 previous works in other culture conditions, such as the use of PMMY medium (Jami et al. 2010b). The
685 number of total identified proteins in the said study was greater than in the present work (328, as opposed
686 to 124). However, the percentage of proteins related to plant cell wall degradation was remarkably lower
687 (11.59%, versus the 47.31% reported in our study). PMMY medium does not include plant-derived
688 compounds, whereas the M-SBP medium employed in the present work contains the lignocellulosic
689 substrate SBP as a carbon source. The higher presence of lignocellulolytic enzymes in the extracts
690 recovered after cultivation on SBP indicates the influence of plant-derived carbon sources as inducers
691 of these enzymatic groups. Previous works have found high percentages of fungal- secreted CAZymes
692 when inducing substrates derived from plants were used (Adav et al. 2012; Dilokpimol et al. 2020; Liu
693 et al. 2013; Song et al. 2016).

694 Among the proteins identified by Jami and co-workers in *P. rubens* Wisconsin 54–1255 secretome, there
695 was PrFaeA (Pc20g07010), which was not identified in this work when analyzing enzyme extracts
696 produced by *P. rubens* B13 grown on SBP (Jami et al. 2010b). This may be explained by the fact that
697 the B13 transformant does not overexpress PrFaeA but PrFaeB (Pc12g08300), and the endogenous
698 PrFaeA, being a type A FAE, is not successfully induced by SBP (Crepin et al. 2004). On the other

699 hand, PrFaeB was not identified in the study performed by Jami and co-workers, whereas 4 isoforms
700 were found in the present work, presumably because of the use of SBP and the analysis of a different *P.*
701 *rubens* strain (in this case, the B13 transformant, which is capable of overexpressing PrFaeB).

702 Some of the identified proteins involved in the degradation of plant cell walls were cellulases,
703 hemicellulases, and pectinases. The presence of enzymes capable of degrading matrix polysaccharides
704 may be due to the polysaccharide composition of SBP, which was used as an inducing substrate and has
705 a high content of hemicelluloses and pectins (Hutnan et al. 2000; Mardones et al. 2019; Micard et al.
706 1996; Oleas et al. 2017). A strong representation of these groups of hydrolases has been reported in an
707 extracellular proteome study of the fungal strain *A. alternata* PDA1, grown on exactly the same
708 lignocellulosic substrate (García-Calvo et al. 2018). The presence of several xylanolytic enzymes in
709 *Penicillium* spp. has been determined in previous studies, which have identified and characterized
710 CAZymes such as endoxylanases, β -xylosidases, arabinofuranosidases, acetyl xylan esterases, as well
711 as FAEs (the latter belonging to species such as *P. expansum*, *P. funiculosum*, *P. pinophilum*, *P.*
712 *purpurogenum*, and *P. subrubescens*). The studies on the two novel enzymes with FAE activity carried
713 out in the present work (PrFaeA and PrFaeB, from *P. rubens* Wisconsin 54–1255) contribute to the
714 understanding of the xylanolytic enzymatic system from the genus *Penicillium* (Dilokpimol et al. 2020;
715 Donaghy and McKay 1995; Kroon et al. 2000; Mardones et al. 2019; Oleas et al. 2017; Schneider et al.
716 2016).

717 The *P. rubens* B13 enzyme extracts studied in the present work were capable of catalyzing the release
718 of ferulic acid from the natural substrate SBP, extracting approximately 22.7–41.7% (w/w) of the total
719 ferulic acid content using very limited quantities of enzyme extract (Benoit et al. 2006; García-Calvo et
720 al. 2018; López Alonso et al. 2011; Micard et al. 1996). Other *Penicillium* sp. strains have demonstrated
721 the ability to release this hydroxycinnamic acid from natural substrates, such as *P. chrysogenum* 31B,
722 which showed optimum FAE conditions at 50 and pH 6.0–7.0 and extracted approximately up to 85%
723 (w/w) of the alkaline extractable ferulic acid in SBP (Sakamoto et al. 2005). In general, previously
724 described fungal FAEs show great variations in their physiochemical characteristics (molecular weight,
725 isoelectric point, pH, and temperature optima). This is likely related to the different origins of FAEs,
726 which have evolved from highly divergent families of enzymes (Dilokpimol et al. 2016). Fungal FAEs
727 are active from pH 3.0 to 10.0 and 20 to 75 °C, even though optimal activity values are usually at pH
728 4.0–7.0 and temperatures below 50–55 °C (Dilokpimol et al. 2016; Fazary and Ju 2007; Koseki et al.
729 2009a; Topakas et al. 2007; Wang et al. 2016a). To the best of our knowledge, no correlation has been
730 observed between the physiochemical characteristics of the FAEs and their optimal reaction conditions.
731 The results obtained in the present study fall within the optimal activity ranges of other fungal enzymes
732 with FAE activity consulted in the literature.

733 Although the main interest in *P. rubens* Wisconsin 54–1255 has traditionally been due to its role as an
734 antibiotic producer, its powerful mechanism for the degradation of plant biomass represents an

735 interesting source of lignocellulolytic enzymes. A study published by van den Brink and de Vries in
736 2011 indicated the putative presence of several CAZymes in the *P. rubens* Wisconsin 54–1255 genome,
737 including as many as 158 glycoside hydrolases (GHs), 7 carbohydrate esterases (CEs), and 9
738 polysaccharide lyases (PLs) (van den Brink and de Vries 2011). According to the Carbohydrate Active
739 Enzymes database as of 23rd August 2022 (CAZy; [http:// www. cazy. org](http://www.cazy.org)), the number of putative
740 CAZymes in this fungal strain could in fact be greater, including up to 230 putative sequences of GHs,
741 21 CEs and 10 PLs (Drula et al. 2022). The identification of several CAZymes in the *P. rubens* B13
742 partial secreted proteome analysis, as well as the detected lignocellulolytic activities, confirms *P. rubens*
743 B13 as a fungal strain with promising applications in the degradation of lignocellulose.

744 The untargeted metabolite analyses performed in the present work constitute a useful initial approach to
745 identify putative bioactive molecules that could hinder the industrial applicability of the enzyme
746 extracts. The verification of the putative annotations is challenging and depends on the availability of
747 standards and MS/MS fragmentation patterns libraries. In this regard, efforts are being made to facilitate
748 the reliability of the annotations, such as the creation of open-access databases including extensive
749 MS/MS information (Creek et al. 2014; Degnes et al. 2017; Wang et al. 2016b; Zhu et al. 2013). The
750 metabolites that were putatively annotated from the analyzed *P. rubens* B13 samples included a
751 mycotoxin and two antibiotics. The putative mycotoxin, aflatoxin B1, was found in both the enzyme
752 samples originating from the M-SBP cultures and in the M-SBP medium. Since *P. rubens* is not among
753 the known aflatoxin B1 producers (*Aspergillus* spp.) (Frisvad et al. 2005; Tola and Kebede 2016), this
754 toxin was most likely produced by other fungal species during storage of the natural plant derivative
755 SBP. Thus, the putative identification of this mycotoxin in the analyzed samples is not necessarily an
756 obstacle to the commercialization of the enzyme extracts. Furthermore, the identification was
757 qualitative, and the levels of this mycotoxin could be compliant with the EU mycotoxins limits and
758 regulations (McEvoy 2016; van Egmond et al. 2007; Vila-Donat et al. 2018). Regarding antibiotics,
759 penicillin G was putatively identified in samples from cultivations on M-SBP and M-OAT media,
760 whereas penicillin V was only found in M-OAT. Although these antibiotics were putatively identified
761 in cultivation broths, they were not found in the enzyme extracts. Given that enzyme extracts are more
762 suitable for commercialization than raw cultivation broths, this finding is favorable toward its industrial
763 applicability. The presence of limited amounts of antibiotics in the mentioned extracts would be
764 problematic, as it could lead to the appearance of allergies and bacterial antibiotic resistance, which is
765 an increasing global concern (Franco et al. 2009; Laich et al. 2002; Lobanovska and Pilla 2017; Ventola
766 2015). These findings should be taken into consideration, and further analyses are advisable to ensure
767 the safety of the use of the enzyme extracts, concerning mycotoxin levels and bioactivity. The putative
768 presence of undesirable bioactive compounds in the enzyme extracts may also be avoided by means of
769 heterologous enzyme production in GRAS expression platforms, such as other filamentous fungi, yeast,
770 or bacteria (Sewalt et al. 2016). Furthermore, another alternative to prevent the presence of undesirable
771 metabolites would be targeted knockouts in the biosynthesis of the actual compounds by the employment

772 of molecular engineering techniques such as CRISPR-Cas9-based genome editing, which has been
773 developed and successfully applied to *P. rubens* (Pohl et al. 2016).

774 The genetic engineering techniques and proteomic approaches carried out in this work increase the
775 knowledge of the renowned penicillin producer *P. rubens* (formerly, *Penicillium chrysogenum*)
776 Wisconsin 54–1255 cultivated in conditions that lead to the production of plant cell wall degrading
777 enzymes. Several enzymatic activities and putative lignocellulolytic enzymes were detected in the
778 enzyme extracts obtained from this fungal strain, including cellulases, hemicellulases, and pectinases.
779 These findings point to *P. rubens* Wisconsin 54–1255 as a novel source of lignocellulolytic enzymes to
780 be taken into consideration for further studies.

781 The present work identified two sequences in the genome of *P. rubens* Wisconsin 54–1255 encoding
782 putative FAEs, according to their homology to *Aspergillus* sp. FAEs (ORFs Pc20g07010 and
783 Pc12g08300, encoding the putative FAEs PrFaeA and PrFaeB, respectively). The overexpression of
784 PrFaeA and PrFaeB, followed by FAE activity assays, confirmed their FAE activity. To our knowledge,
785 this constitutes the first report of FAE activity in the aforementioned gene products.

786 Furthermore, the PrFaeB overexpressing strain obtained and studied in this work (*P. rubens* B13) is a
787 promising candidate for further studies on FAEs and potential industrial applications, considering its
788 FAE activity and suitability for scale-up of the cultivations. The FAE activity detected in its enzyme
789 extract, which surpassed that of the analyzed commercial preparations, has potential applications in
790 industries such as food, feed, pulp and paper, cosmetics, pharmaceuticals, food, feed, and biofuels.

791 **Supplementary Information** The online version contains supplementary material available at
792 <https://doi.org/10.1007/s00253-022-12335-w>.

793 **Acknowledgements** The authors want to thank the Spanish Ministry of Economy, Industry and
794 Competitiveness (MINECO) for funding the project (ref. no. CTM2012-32026) and awarding Ms. Laura
795 García-Calvo with a PhD grant (ref. no. BES-2013-064578) and international stay grant (ref. no. EEBB-
796 I-16-11760).

797 The authors also want to thank the European Union program ERAIB 7th Joint Call [ProWood project
798 (Wood and derivatives protection by novel bio-coating solutions, ERA-IB-16-040)] through the APCIN
799 call of the Spanish Ministry of Economy, Industry and Competitiveness and the State Research Agency
800 (AEI) (Project ID: PCIN-2016- 081). Special thanks to the ESTELLA project (“DESIGN of bio-based
801 Thermoset polymer with rEcyCLing capabiLity by dynAmic bonds for bio-composite manufacturing”)
802 (Project no.: 101058371) funded by the European Union through the Horizon Europe Framework
803 Programme (call: HORIZON-CL4-2021-RESILIENCE-01-11). The funding sources had no
804 involvement in the study design; collection, analysis, and interpretation of data; writing of the report;
805 and decision to submit the article for publication. We would also like to thank all the members of

806 INBIOTEC (Spain) and SINTEF Biotechnology and Nanomedicine (Norway), as well as the University
807 of León (Spain), for their collaboration and invaluable help aiding in the completion of this work.

808 **Author contribution** LGC, RRC, RVU, SMA, HS, and CB conceived and designed research. LGC,
809 RRC, MFA, CMV, KFD, and CB conducted experiments. LGC, RRC, KFD, and CB analyzed data and
810 contributed to visualization. LGC and RRC wrote the original draft. LGC, RVU, SMA, KFD, HS, and
811 CB reviewed and edited the draft. All authors read and approved the manuscript. RVU, HS, and CB
812 acquired resources and funding.

813 **Funding** This study was funded by a project (ref. no. CTM2012-32026) of the Spanish Ministry of
814 Economy, Industry and Competitiveness (MINECO) and co-funded by the ERDF (European Regional
815 Development Fund). Ms. Laura García-Calvo was supported by a PhD grant (ref. no. BES-2013–
816 064578) and an international stay grant (ref. no. EEBB-I-16–11760), awarded by the Spanish Ministry
817 MINECO.

818 **Data availability** Data is available in the article’s Supplementary material. Additional data and
819 biological material are available on request from the authors. The data that support the findings of this
820 study are available from the corresponding authors (Carlos Barreiro and Ricardo V. Ullán), upon
821 reasonable request.

822 **Declarations**

823 **Competing interests** The authors declare no competing interests.

824 **References**

825 Adav SS, Ravindran A, Sze SK (2012) Quantitative proteomic analysis of lignocellulolytic enzymes by
826 *Phanerochaete chrysosporium* on different lignocellulosic biomass. *J Proteomics* 75(5):1493–1504.
827 <https://doi.org/10.1016/j.jprot.2011.11.020>

828 Alam MA, Subhan N, Hossain H, Hossain M, Reza HM, Rahman MM, Ullah MO (2016)
829 Hydroxycinnamic acid derivatives: a potential class of natural compounds for the management of lipid
830 metabolism and obesity. *Nutr Metab* 13(1):1–13. <https://doi.org/10.1186/s12986-016-0080-3>

831 Almagro Armenteros JJ, Tsirigos KD, Sønderby CK, Petersen TN, Winther O, Brunak S, von Heijne G,
832 Nielsen H (2019) SignalP 5.0 improves signal peptide predictions using deep neural networks. *Nat*
833 *Biotechnol* 37(4):420–423. <https://doi.org/10.1038/s41587-019-0036-z>

834 Arnau J, Yaver D, Hjort CM (2020) Strategies and challenges for the development of industrial enzymes
835 using fungal cell factories. pp 179–210

836 Barredo Fuente JL, Rodríguez Saiz M, Moreno Valle MÁ, Collados de la Vieja AJ, Salto Maldonado F,
837 Díez B (1998) Promotores de los genes glutamato deshidrogenasa, β -n-acetilhexosaminidasa Y-actina
838 y su utilizacion en sistemas de expresion, secrecion y antisentido de hongos filamentosos.

839 Barreiro C, Barredo J-L (2021) Worldwide clinical demand for antibiotics: Is it a real countdown? In:
840 Barreiro C, Barredo J-L (eds) Antimicrobial Therapies: Methods and Protocols. Springer, US, New
841 York, NY, pp 3–15.

842 Barreiro C, García-Estrada C, Martín JF (2012a) Proteomics methodology applied to the analysis of
843 filamentous fungi - New trends for an impressive diverse group of organisms. In: Prasain JK (ed). vol
844 78. InTech, Rijeka, Croacia, pp 159–171.

845 Barreiro C, Martín JF, García-Estrada C (2012b) Proteomics shows new faces for the old penicillin
846 producer *Penicillium chrysogenum*. J Biomed Biotechnol 2012b:ID 105109, 1–15
847 <https://doi.org/10.5772/31320>

848 Bendtsen JD, Jensen LJ, Blom N, von Heijne G, Brunak S (2004) Feature-based prediction of non-
849 classical and leaderless protein secretion. Protein Eng Des Sel 17(4):349–356.
850 <https://doi.org/10.1093/protein/gzh037>

851 Benoit I, Navarro D, Marnet N, Rakotomanomana N, Lesage-Meessen L, Sigoillot J-C, Asther M,
852 Asther M (2006) Feruloyl esterases as a tool for the release of phenolic compounds from agro-industrial
853 by-products. Carbohydr Res 341(11):1820–1827. <https://doi.org/10.1016/j.carres.2006.04.020>

854 Bhatnagar D, Yu J, Ehrlich KC (2002) Toxins of filamentous fungi. Chem Immunol 81:167–206.
855 <https://doi.org/10.1159/000058867>

856 Boratyn GM, Camacho C, Cooper PS, Coulouris G, Fong A, Ma N, Madden TL, Matten WT, McGinnis
857 SD, Merezhuk Y, Raytselis Y, Sayers EW, Tao T, Ye J, Zaretskaya I (2013) BLAST: a more efficient
858 report with usability improvements. Nucleic Acids Res 41(Web Server issue):W29–33
859 <https://doi.org/10.1093/nar/gkt282>

860 Bradford MM (1976) A rapid and sensitive method for the quantitation of microgram quantities of
861 protein utilizing the principle of protein-dye binding. Anal Biochem 72(1–2):248–254.
862 [https://doi.org/10.1016/0003-2697\(76\)90527-3](https://doi.org/10.1016/0003-2697(76)90527-3)

863 Braga CMP, Delabona PdS, Lima DJdS, Paixão DAA, Pradella JGdC, Farinas CS (2014) Addition of
864 feruloyl esterase and xylanase produced on-site improves sugarcane bagasse hydrolysis. Bioresour
865 Technol 170:316–324. <https://doi.org/10.1016/j.biortech.2014.07.115>

866 Candiano G, Bruschi M, Musante L, Santucci L, Ghiggeri GM, Carnemolla B, Orecchia P, Zardi L,
867 Righetti PG (2004) Bluesilver: a very sensitive colloidal Coomassie G-250 staining for proteome
868 analysis. Electrophoresis 25(9):1327–1333. <https://doi.org/10.1002/elps.200305844>

869 Casqueiro J, Banuelos O, Gutierrez S, Hijarrubia MJ, Martín JF (1999) Intrachromosomal
870 recombination between direct repeats in *Penicillium chrysogenum*: gene conversion and deletion events.
871 Mol Gen Genet 261(6):994–1000. <https://doi.org/10.1007/s004380051048>

872 Castanares A, McCrae SI, Wood TM (1992) Purification and properties of a feruloyl/p-coumaroyl
873 esterase from the fungus *Penicillium pinophilum*. *Enzyme Microb Technol* 14(11):875–884.
874 [https://doi.org/10.1016/0141-0229\(92\)90050-X](https://doi.org/10.1016/0141-0229(92)90050-X)

875 Chapman J, Ismail A, Dinu C (2018) Industrial applications of enzymes: Recent advances, techniques,
876 and outlooks. *Catalysts* 8(6):238–238. <https://doi.org/10.3390/catal8060238>

877 Chávez R, Bull P, Eyzaguirre J (2006) The xylanolytic enzyme system from the genus *Penicillium*. *J*
878 *Biotechnol* 123(4):413–433. <https://doi.org/10.1016/j.jbiotec.2005.12.036>

879 Cleveland TE, Dowd PF, Desjardins AE, Bhatnagar D, Cotty PJ (2003) United States Department of
880 Agriculture – Agricultural Research Service research on pre-harvest prevention of mycotoxins and
881 mycotoxigenic fungi in US crops. *Pest Manage Sci* 59(6–7):629–642. <https://doi.org/10.1002/ps.724>

882 Creek DJ, Dunn WB, Fiehn O, Griffin JL, Hall RD, Lei Z, Mistrik R, Neumann S, Schymanski EL,
883 Sumner LW, Trengove R, Wolfender J-L (2014) Metabolite identification: are you sure? And how do
884 your peers gauge your confidence? *Metabolomics* 10:350–353. <https://doi.org/10.1007/s11306-014->
885 0656-8

886 Crepin VF, Faulds CB, Connerton IF (2004) Functional classification of the microbial feruloyl esterases.
887 *Appl Microbiol Biotechnol* 63(6):647–652. <https://doi.org/10.1007/s00253-003-1476-3>

888 Dashtban M, Schraft H, Qin W (2009) Fungal bioconversion of lignocellulosic residues; opportunities
889 & perspectives. *Int J Biol Sci* 5(6):578–595. <https://doi.org/10.7150/ijbs.5.578>

890 de Oliveira DM, Finger-Teixeira A, Rodrigues Mota T, Salvador VH, Moreira-Vilar FC, Correa
891 Molinari HB, Craig Mitchell RA, Marchiosi R, Ferrarese-Filho O, Dantas dos Santos W (2015) Ferulic
892 acid: a key component in grass lignocellulose recalcitrance to hydrolysis. *Plant Biotechnol J* 13:1224–
893 1232. <https://doi.org/10.1111/pbi.12292>

894 de Vries RP, Pa VanKuyk, Kester HCM, Visser J (2002) The *Aspergillus niger faeB* gene encodes a
895 second feruloyl esterase involved in pectin and xylan degradation and is specifically induced in the
896 presence of aromatic compounds. *Biochem J* 363(Pt 2):377–386. <https://doi.org/10.1042/0264->
897 6021:3630377

898 Degnes KF, Kvitvang HFN, Haslene-Hox H, Aasen IM (2017) Changes in the profiles of metabolites
899 originating from protein degradation during ripening of dry cured ham. *Food Bioprocess Technol*
900 10(6):1122–1130. <https://doi.org/10.1007/s11947-017-1894-3>

901 Díez B, Rodríguez-Sáiz M, la Fuente JL, Moreno MÁN, Barredo JL (2005) The *nagA* gene of
902 *Penicillium chrysogenum* encoding β - N -acetylglucosaminidase. *FEMS Microbiol Lett* 242(2):257–
903 264. <https://doi.org/10.1016/j.femsle.2004.11.017>

904 Dilokpimol A, Mäkelä MR, Aguilar-Pontes MV, Benoit-Gelber I, Hildén KS, de Vries RP (2016)
905 Diversity of fungal feruloyl esterases: updated phylogenetic classification, properties, and industrial
906 applications. *Biotechnol Biofuels* 9(1):231–231. <https://doi.org/10.1186/s13068-016-0651-6>

907 Dilokpimol A, Mäkelä MR, Mansouri S, Belova O, Waterstraat M, Bunzel M, Vries RPD, Hildén KS
908 (2017) Expanding the feruloyl esterase gene family of *Aspergillus niger* by characterization of a feruloyl
909 esterase, FaeC. *N Biotechnol* 37:200–209. <https://doi.org/10.1016/j.nbt.2017.02.007>

910 Dilokpimol A, Peng M, Di Falco M, Chin AWT, Hegi RMW, Granchi Z, Tsang A, Hilden KS, Makela
911 MR, de Vries RP (2020) *Penicillium subrubescens* adapts its enzyme production to the composition of
912 plant biomass. *Bioresour Technol* 311:123477. <https://doi.org/10.1016/j.biortech.2020.123477>

913 Domínguez-Santos R, Kosalková K, García-Estrada C, Barreiro C, Ibáñez A, Morales A, Martín J-F
914 (2017) Casein phosphopeptides and CaCl₂ increase penicillin production and cause an increment in
915 microbody/peroxisome proteins in *Penicillium chrysogenum*. *J Proteomics* 156:52–62.
916 <https://doi.org/10.1016/j.jprot.2016.12.021>

917 Donaghy JA, McKay AM (1994) Novel screening assay for the detection of phenolic acid esterases.
918 *World J Microbiol Biotechnol* 10(1):41–44. <https://doi.org/10.1007/BF00357561>

919 Donaghy JA, McKay AM (1995) Production of feruloyl/rho-coumaroyl esterase activity by *Penicillium*
920 *expansum*, *Penicillium brevicompactum* and *Aspergillus niger*. *J Appl Bacteriol* 79(6):657–662.

921 Donaghy J, Kelly PF, McKay AM (1998) Detection of ferulic acid esterase production by *Bacillus* spp.
922 and lactobacilli. *Appl Microbiol Biotechnol* 50:257–260. <https://doi.org/10.1007/s002530051286>

923 Drula E, Garron M-L, Dogan S, Lombard V, Henrissat B, Terrapon N (2022) The carbohydrate-active
924 enzyme database: functions and literature. *Nucleic Acids Res* 50(D1):D571–D577.
925 <https://doi.org/10.1093/nar/gkab1045>

926 Escamilla-Alvarado C, Pérez-Pimienta JA, Ponce-Noyola T, Poggi-Varaldo HM (2017) An overview
927 of the enzyme potential in bioenergy-producing biorefineries. *J Chem Technol Biotechnol* 92(5):906–
928 924. <https://doi.org/10.1002/jctb.5088>

929 Faulds CB (2010) What can feruloyl esterases do for us? *Phytochem Rev* 9(1):121–132.
930 <https://doi.org/10.1007/s11101-009-9156-2>

931 Faulds CB, Zanichelli D, Crepin VF, Connerton IF, Juge N, Bhat MK, Waldron KW (2003) Specificity
932 of feruloyl esterases for waterextractable and water-unextractable feruloylated polysaccharides:
933 influence of xylanase. *J Cereal Sci* 38(3):281–288. [https://doi.org/10.1016/S0733-5210\(03\)00029-8](https://doi.org/10.1016/S0733-5210(03)00029-8)

934 Fazary AE, Ju Y-H (2007) Feruloyl esterases as biotechnological tools: current and future perspectives.
935 *Acta Biochim Biophys Sin* 39(11):811–828. <https://doi.org/10.1111/j.1745-7270.2007.00348.x>

936 Fazary AE, Ju Y-H (2008) The large-scale use of feruloyl esterases in industry. *Biotechnol Mol Biol*
937 3(5):95–110.

938 Fernández-Aguado M, Martín JF, Rodríguez-Castro R, García-Estrada C, Albillos SM, Teijeira F, Ullán
939 RV (2014) New insights into the isopenicillin N transport in *Penicillium chrysogenum*. *Metab Eng*
940 22:89–103. <https://doi.org/10.1016/j.ymben.2014.01.004>

941 Fierro F, Vaca I, Castillo NI, García-Rico RO, Chávez R (2022) *Penicillium chrysogenum*, a vintage
942 model with a cutting-edge profile in Biotechnology. *Microorganisms* 10(3):573–573.
943 <https://doi.org/10.3390/microorganisms10030573>

944 Franco BE, Martínez MA, Sánchez Rodríguez MA, Wertheimer AI (2009) The determinants of the
945 antibiotic resistance process. *Infect Drug Resist* 2(1):1–11. <https://doi.org/10.2147/IDR.S4899>

946 Frisvad JC, Skouboe P, Samson RA (2005) Taxonomic comparison of three different groups of aflatoxin
947 producers and a new efficient producer of aflatoxin B₁, sterigmatocystin and 3-O-
948 methylsterigmatocystin, *Aspergillus rambellii* sp. nov. *Syst Appl Microbiol* 28(5):442–453.
949 <https://doi.org/10.1016/j.syapm.2005.02.012>

950 García-Calvo L, Ullán RV, Fernández-Aguado M, García-Lino AM, Balaña-Fouce R, Barreiro C (2018)
951 Secreted protein extract analyses present the plant pathogen *Alternaria alternata* as a suitable industrial
952 enzyme toolbox. *J Proteomics* 177:48–64. <https://doi.org/10.1016/j.jprot.2018.02.012>

953 García-Estrada C, Ullán RV, Albillos SM, Fernández-Bodega MÁ, Durek P, Von Döhren H, Martín JF
954 (2011) A single cluster of coregulated genes encodes the biosynthesis of the mycotoxins roquefortine C
955 and meleagrín in *Penicillium chrysogenum*. *Chem Biol* 18(11):1499–1512.
956 <https://doi.org/10.1016/j.chembiol.2011.08.012>

957 García-Estrada C, Martín JF, Cueto L, Barreiro C (2020) Omics approaches applied to *Penicillium*
958 *chrysogenum* and penicillin production: revealing the secrets of improved productivity. *Genes*
959 11(6):712–712. <https://doi.org/10.3390/genes11060712>

960 Garre V, Müller U, Tudzynski P (1998) Cloning, characterization, and targeted disruption of *cpcat1*,
961 Coding for an in planta secreted catalase of *Claviceps purpurea*. *Mol Plant-Microbe Interact* 11(8):772–
962 783. <https://doi.org/10.1094/MPMI.1998.11.8.772>

963 Ghose TK (1987) Measurement of cellulase activities. *Pure & Appl Chem* 59(2):257–268.

964 Gifre L, Arís A, Bach À, Garcia-Fruitós E (2017) Trends in recombinant protein use in animal
965 production. *Microb Cell Factories* 16(1):40–40. <https://doi.org/10.1186/s12934-017-0654-4>

966 Gopalan N, Rodríguez-Duran LV, Saucedo-Castaneda G, Nampoothiri KM (2015) Review on
967 technological and scientific aspects of feruloyl esterases: a versatile enzyme for biorefining of biomass.
968 *Bioresour Technol* 193:534–544. <https://doi.org/10.1016/j.biortech.2015.06.117>

969 Guerriero G, Hausman J-F, Strauss J, Ertan H, Siddiqui KS (2016) Lignocellulosic biomass:
970 biosynthesis, degradation, and industrial utilization. *Eng Life Sci* 16(1):1–16.
971 <https://doi.org/10.1002/elsc.201400196>

972 Gutiérrez S, Díez B, Alvarez E, Barredo JL, Martín JF (1991) Expression of the *penDE* gene of
973 *Penicillium chrysogenum* encoding isopenicillin N acyltransferase in *Cephalosporium acremonium*:
974 production of benzylpenicillin by the transformants. *Mol Gen Genet* 225(1):56–64.

975 Hanahan D (1983) Studies on transformation of *Escherichia coli* with plasmids. *J Mol Biol* 166(4):557–
976 580. [https://doi.org/10.1016/S0022-2836\(83\)80284-8](https://doi.org/10.1016/S0022-2836(83)80284-8)

977 Havliš J, Thomas H, Šebela M, Shevchenko A (2003) Fast-response proteomics by accelerated in-gel
978 digestion of proteins. *Anal Chem* 75(6):1300–1306. <https://doi.org/10.1021/ac026136s>

979 Hermoso JA, Sanz-Aparicio J, Molina R, Juge N, González R, Faulds CB (2004) The crystal structure
980 of feruloyl esterase A from *Aspergillus niger* suggests evolutive functional convergence in feruloyl
981 esterase family. *J Mol Biol* 338(3):495–506. <https://doi.org/10.1016/j.jmb.2004.03.003>

982 Houbraken J, Frisvad JC, Samson RA (2011) Fleming’s penicillin producing strain is not *Penicillium*
983 *chrysogenum* but *P. rubens*. *IMA Fungus* 2(1):87–95. <https://doi.org/10.5598/imafungus.2011.02.01.12>

984 Huerta-Cepas J, Szklarczyk D, Heller D, Hernández-Plaza A, Forslund SK, Cook H, Mende DR, Letunic
985 I, Rattei T, Jensen LJ, von Mering C, Bork P (2019) eggNOG 50: a hierarchical, functionally and
986 phylogenetically annotated orthology resource based on 5090 organisms and 2502 viruses. *Nucleic*
987 *Acids Res* 47(D1):D309–D314. <https://doi.org/10.1093/nar/gky1085>

988 Hutnan M, Dřitl M, Mrfatkova L (2000) Anaerobic biodegradation of sugar beet pulp. *Biodegradation*
989 11:203–211.

990 Jäger G, Büchs J (2012) Biocatalytic conversion of lignocellulose to platform chemicals. *Biotechnol J*
991 7(9):1122–1136. <https://doi.org/10.1002/biot.201200033>

992 Jami M-S, Barreiro C, García-Estrada C, Martín J-F (2010a) Proteome analysis of the penicillin
993 producer *Penicillium chrysogenum*. *Mol Cell Proteomics* 9(6):1182–1198.
994 <https://doi.org/10.1074/mcp.M900327-MCP200>

995 Jami M-S, García-Estrada C, Barreiro C, Cuadrado A-A, Salehi-Najafabadi Z, Martín J-F (2010b) The
996 *Penicillium chrysogenum* extracellular proteome Conversion from a food-rotting strain to a versatile cell
997 factory for white biotechnology. *Mol Cell Proteomics* 9(12):2729–2744.
998 <https://doi.org/10.1074/mcp.M110.001412>

999 Jami M-S, Martín J-F, Barreiro C, Domínguez-Santos R, Vasco-Cárdenas M-F, Pascual M, García-
1000 Estrada C (2018) Catabolism of phenylacetic acid in *Penicillium rubens* Proteome-wide análisis in
1001 response to the benzylpenicillin side chain precursor. *J Proteomics* 187(1):243–259.

1002 Jimenez-Flores R, Fake G, Carroll J, Hood E, Howard J (2010) A novel method for evaluating the
1003 release of fermentable sugars from cellulosic biomass. *Enzyme Microb Technol* 47(5):206–211.
1004 <https://doi.org/10.1016/j.enzmictec.2010.07.003>

1005 Kiel JAKW, van den Berg MA, Fusetti F, Poolman B, Bovenberg RAL, Veenhuis M, van der Klei IJ
1006 (2009) Matching the proteome to the genome: the microbody of penicillin-producing *Penicillium*
1007 *chrysogenum* cells. *Funct Integr Genomics* 9(2):167–184. <https://doi.org/10.1007/s10142-009-0110-6>

1008 Kosalková K, García-Estrada C, Ullán RV, Godio RP, Feltrer R, Teijeira F, Mauriz E, Martín JF (2009)
1009 The global regulator LaeA controls penicillin biosynthesis, pigmentation and sporulation, but not
1010 roquefortine C synthesis in *Penicillium chrysogenum*. *Biochimie* 91(2):214–225.
1011 <https://doi.org/10.1016/j.biochi.2008.09.004>

1012 Koseki T, Furuse S, Iwano K, Matsuzawa H (1998) Purification and characterization of a feruloyl
1013 esterase from *Aspergillus awamori*. *Biosci, Biotechnol, Biochem* 62(10):2032–2034.

1014 Koseki T, Fushinobu S, Ardiansyah SH, Komai M (2009a) Occurrence, properties, and applications of
1015 feruloyl esterases. *Appl Microbiol Biotechnol* 84(5):803–810. <https://doi.org/10.1007/s00253-009-2148-8>

1016

1017 Koseki T, Hori A, Seki S, Murayama T, Shiono Y (2009b) Characterization of two distinct feruloyl
1018 esterases, AoFaeB and AoFaeC, from *Aspergillus oryzae*. *Appl Microbiol Biotechnol* 83(4):689–696.
1019 <https://doi.org/10.1007/s00253-009-1913-z>

1020 Kroon PA, Williamson G, Fish NM, Archer DB, Belshaw NJ (2000) A modular esterase from
1021 *Penicillium funiculosum* which releases ferulic acid from plant cell walls and binds crystalline cellulose
1022 contains a carbohydrate binding module. *Eur J Biochem* 267(23):6740–6752.
1023 <https://doi.org/10.1046/j.1432-1327.2000.01742.x>

1024 Kühnel S, Pouvreau L, Appeldoorn MM, Hinz SWA, Schols HA, Gruppen H (2012) The ferulic acid
1025 esterases of *Chrysosporium lucknowense* C1: purification, characterization and their potential
1026 application in biorefinery. *Enzyme Microb Technol* 50(1):77–85.
1027 <https://doi.org/10.1016/j.enzmictec.2011.09.008>

1028 Kumar CG, Kamle A, Mongolla P, Joseph J (2011) Parametric optimization of feruloyl esterase
1029 production from *Aspergillus terreus* strain GA2 isolated from tropical agro-ecosystems cultivating sweet
1030 sorghum. *J Microbiol Biotechnol* 21(9):947–953. <https://doi.org/10.4014/jmb.1104.04014>

1031 Kumar V, Singh D, Sangwan P, Gill pk (2014) Global market scenario of industrial enzymes. In:
1032 Beniwal V, Sharma AK (eds). Nova Science Publishers, Nueva York, EEUU, pp 173–196.

1033 Laich F, Fierro F, Martin JF (2002) Production of penicillin by fungi growing on food products:
1034 Identification of a complete penicillin gene cluster in *Penicillium griseofulvum* and a truncated cluster

1035 in *Penicillium verrucosum*. Appl Environ Microbiol 68(3):1211–1219.
1036 <https://doi.org/10.1128/AEM.68.3.1211-1219.2002>

1037 Li C, Lin F, Li Y, Wei W, Wang H, Qin L, Zhou Z, Li B, Wu F, Chen Z (2016) A β -glucosidase hyper-
1038 production *Trichoderma reesei* mutant reveals a potential role of cel3D in cellulase production. Microb
1039 Cell Factories 15(1):151–151. <https://doi.org/10.1186/s12934-016-0550-3>

1040 Liu G, Zhang L, Wei X, Zou G, Qin Y, Ma L, Li J, Zheng H, Wang S, Wang C, Xun L, Zhao G-P, Zhou
1041 Z, Qu Y (2013) Genomic and secretomic analyses reveal unique features of the lignocellulolytic enzyme
1042 system of *Penicillium decumbens*. PLoS ONE 8(2):e55185–e55185.
1043 <https://doi.org/10.1371/journal.pone.0055185>

1044 Lobanovska M, Pilla G (2017) Penicillin's discovery and antibiotic resistance: Lessons for the future?
1045 Yale J Biol Med 90(1):135–145.

1046 López Alonso R, Ramírez de Lara C, Rivero L, Ruiz AE, Torres Zapata CT, Ullán RV (2011) Aplicación
1047 de una nueva FAE en la liberación químico-enzimática de ácido ferúlico a partir de pulpa de remolacha.
1048 Cienc Agron 19(21–25):2250–8872.

1049 De Lucca AJ (2007) Harmful fungi in both agriculture and medicine. Rev Iberoam Micol 24(1):3–13
1050 20072403 [pii] ET - 2007/06/27.

1051 Lutzoni F, Kauff F, Cox CJ, McLaughlin D, Celio G, Dentinger C, Padamsee M, Hibbett D, James TY,
1052 Baloch E, Grube M, Reeb V, Hofstetter V, Schoch C, Arnold AE, Miadlikowska J, Spatafora J, Johnson
1053 D, Hambleton S, Crockett M, Shoemaker R, Sung GH, Lücking R, Lumbsch T, O'Donnell K, Binder
1054 M, Diederich P, Ertz D, Gueidan C, Hansen K, Harris RC, Hosaka K, Lim YW, Matheny B, Nishida H,
1055 Pfister D, Rogers J, Rossman A, Schmitt I, Sipman H, Stone J, Sugiyama J, Yahr R, Vilgalys R (2004)
1056 Assembling the fungal tree of life: Progress, classification, and evolution of subcellular traits. Am J Bot
1057 91(10):1446–1480. <https://doi.org/10.3732/ajb.91.10.1446>

1058 Lynd LR, Weimer PJ, van Zyl WH, Pretorius IS (2002) Microbial cellulose utilization: fundamentals
1059 and biotechnology. Microbiol Mol Biol Rev 66(3):506–577. [https://doi.org/10.1128/MMBR.66.3.506-](https://doi.org/10.1128/MMBR.66.3.506-577.2002)
1060 [577.2002](https://doi.org/10.1128/MMBR.66.3.506-577.2002)

1061 Mäkelä MR, Donofrio N, De Vries RP (2014) Plant biomass degradation by fungi. Fungal Genet Biol
1062 72:2–9. <https://doi.org/10.1016/j.fgb.2014.08.010>

1063 Mäkelä MR, Dilokpimol A, Koskela SM, Kuuskeri J, de Vries RP, Hildén K (2018) Characterization of
1064 a feruloyl esterase from *Aspergillus terreus* facilitates the division of fungal enzymes from Carbohydrate
1065 Esterase family 1 of the carbohydrate-active enzymes (CAZy) database. Microb Biotechnol 11(5):869–
1066 880. <https://doi.org/10.1111/1751-7915.13273>

1067 Manisha YSK (2017) Technological advances and applications of hydrolytic enzymes for valorization
1068 of lignocellulosic biomass. *Bioresour Technol* 245:1727–1739.
1069 <https://doi.org/10.1016/j.biortech.2017.05.066>

1070 Mardones W, Callegari E, Eyzaguirre J (2019) Corn cob and sugar beet pulp induce specific sets of
1071 lignocellulolytic enzymes in *Penicillium purpurogenum*. *Mycology* 10(2):118–125.
1072 <https://doi.org/10.1080/21501203.2018.1517830>

1073 Martínez-Gomariz M, Perumal P, Mekala S, Nombela C, Chaffin WL, Gil C (2009) Proteomic analysis
1074 of cytoplasmic and surface proteins from yeast cells, hyphae, and biofilms of *Candida albicans*.
1075 *Proteomics* 9(8):2230–2252. <https://doi.org/10.1002/pmic.200700594>

1076 Mathew S, Abraham TE (2004) Ferulic acid: an antioxidant found naturally in plant cell walls and
1077 feruloyl esterases involved in its release and their applications. *Crit Rev Biotechnol* 24(2–3):59–83.
1078 <https://doi.org/10.1080/07388550490491467>

1079 Mathew S, Abraham TE (2006) Bioconversions of ferulic acid, an hydroxycinnamic acid. *Crit Rev*
1080 *Microbiol* 32(3):115–125. <https://doi.org/10.1080/10408410600709628>

1081 Mattéotti C, Bauwens J, Brasseur C, Tarayre C, Thonart P, Destain J, Francis F, Haubruge E, De Pauw
1082 E, Portetelle D, Vandenberg M (2012) Identification and characterization of a new xylanase from Gram-
1083 positive bacteria isolated from termite gut (*Reticulitermes santonensis*). *Protein Expression Purif*
1084 83(2):117–127. <https://doi.org/10.1016/j.pep.2012.03.009>

1085 McEvoy JDG (2016) Emerging food safety issues: an EU perspective. *Drug Test Anal* 8(5–6):511–520.
1086 <https://doi.org/10.1002/dta.2015>

1087 McLaughlin DJ, Hibbett DS, Lutzoni F, Spatafora JW, Vilgalys R (2009) The search for the fungal tree
1088 of life. *Trends Microbiol* 17(11):488–497. <https://doi.org/10.1016/j.tim.2009.08.001>

1089 Menon V, Rao M (2012) Trends in bioconversion of lignocellulose: biofuels, platform chemicals &
1090 biorefinery concept. *Prog Energy Combust Sci* 38(4):522–550.
1091 <https://doi.org/10.1016/j.pecs.2012.02.002>

1092 Micard V, Renard CMGC, Thibault JF (1996) Enzymatic saccharification of sugar-beet pulp. *Enzyme*
1093 *Microb Technol* 19(3):162–170. [https://doi.org/10.1016/0141-0229\(95\)00224-3](https://doi.org/10.1016/0141-0229(95)00224-3)

1094 Miller JH (1972) *Experiments in molecular genetics*. Cold Spring Harbor Laboratory Press, U.S., Nueva
1095 York, EEUU Mitchell NJ, Bowers E, Hurburgh C, Wu F (2016) Potential economic losses to the US
1096 corn industry from aflatoxin contamination. *Food Additives & Contaminants: Part A* 33(3):540–550.
1097 <https://doi.org/10.1080/19440049.2016.1138545>

1098 Muggia L, Grube M (2018) Fungal diversity in lichens: from extremotolerance to interactions with
1099 Algae. *Life* 8(2):15–15. <https://doi.org/10.3390/life8020015>

1100 Nielsen H (2017) Predicting secretory proteins with SignalP. In: Kihara D (ed) vol 1611. Humana Press,
1101 Nueva York, EEUU, pp 59–73.

1102 Nielsen H, Engelbrecht J, Brunak S, Heijne GV (1997) Identification of prokaryotic and eukaryotic
1103 signal peptides and prediction of their cleavage sites. *Protein Eng* 10:1–6.
1104 <https://doi.org/10.1142/S0129065797000537>

1105 Nuero OM, Reyes F (2002) Enzymes for animal feeding from *Penicillium chrysogenum* mycelial wastes
1106 from penicillin manufacture. *Lett Appl Microbiol* 34(6):413–416. <https://doi.org/10.1046/j.1472-765X.2002.01113.x>

1108 Oleas G, Callegari E, Sepulveda R, Eyzaguirre J (2017) Heterologous expression, purification and
1109 characterization of three novel esterases secreted by the lignocellulolytic fungus *Penicillium*
1110 *purpurogenum* when grown on sugar beet pulp. *Carbohydr Res* 443–444:42–48.
1111 <https://doi.org/10.1016/j.carres.2017.03.014>

1112 Ou S, Kwok K-C (2004) Ferulic acid: pharmaceutical functions, preparation and applications in foods.
1113 *J Sci Food Agric* 84(11):1261–1269. <https://doi.org/10.1002/jsfa.1873>

1114 Patel AK, Singhanian RR, Pandey A (2016) Novel enzymatic processes applied to the food industry. *Curr*
1115 *Opin Food Sci* 7:64–72. <https://doi.org/10.1016/j.cofs.2015.12.002>

1116 Pérez J, Muñoz-Dorado J, de la Rubia T, Martínez J (2002) Biodegradation and biological treatments of
1117 cellulose, hemicellulose and lignin: an overview. *Int Microbiol* 5(2):53–63.
1118 <https://doi.org/10.1007/s10123-002-0062-3>

1119 Perkins DN, Pappin DJC, Creasy DM, Cottrell JS (1999) Probability based protein identification by
1120 searching sequence databases using mass spectrometry data. *Electrophoresis* 20(18):3551–3567.
1121 [https://doi.org/10.1002/\(sici\)1522-2683\(19991201\)20:18%3c3551::aid-elps3551%3e3.0.co;2-2](https://doi.org/10.1002/(sici)1522-2683(19991201)20:18%3c3551::aid-elps3551%3e3.0.co;2-2)

1122 Pfaffl MW (2001) A new mathematical model for relative quantification in real-time RT-PCR. *Nucleic*
1123 *Acids Res* 29(9):45e–445. <https://doi.org/10.1093/nar/29.9.e45>

1124 Phuengmaung P, Sunagawa Y, Makino Y, Kusumoto T, Handa S, Sukhumsirichart W, Sakamoto T
1125 (2019) Identification and characterization of ferulic acid esterase from *Penicillium chrysogenum* 31B:
1126 de-esterification of ferulic acid decorated with L-arabinofuranoses and D-galactopyranoses in sugar beet
1127 pectin. *Enzyme Microb Technol* 131(June):109380–109380.
1128 <https://doi.org/10.1016/j.enzmictec.2019.109380>

1129 Pohl C, Kiel JAKW, Driessen AJM, Bovenberg RAL, Nygård Y (2016) CRISPR/Cas9 based genome
1130 editing of *Penicillium chrysogenum*. *ACS Synth Biol*:acssynbio.6b00082-acssynbio.6b00082
1131 <https://doi.org/10.1021/acssynbio.6b00082>

1132 Poonawalla FM, Patel KL, Iyengar MR (1965) Invertase production by *Penicillium chrysogenum* and
1133 other fungi in submerged fermentation. *Appl Microbiol* 13(5):749–754.

1134 Ralet MC, Faulds CB, Williamson G, Thibault JF (1994) Degradation of feruloylated oligosaccharides
1135 from sugar-beet pulp and wheat bran by ferulic acid esterases from *Aspergillus niger*. Carbohydr Res
1136 263(2):257–269. [https://doi.org/10.1016/0008-6215\(94\)00177-4](https://doi.org/10.1016/0008-6215(94)00177-4)

1137 Rasmussen R (2001) Quantification on the LightCycler. In: Meuer S, Wittwer C, Nakagawara K (eds).
1138 Springer, Berlin, Heidelberg, pp 21–34.

1139 Ravalason H, Grisel S, Chevret D, Favel A, Berrin JG, Sigoillot JC, Herpoël-Gimbert I (2012) *Fusarium*
1140 *verticillioides* secretome as a source of auxiliary enzymes to enhance saccharification of wheat straw.
1141 Bioresour Technol 114:589–596. <https://doi.org/10.1016/j.biortech.2012.03.009>

1142 Record E, Asther M, Sigoillot C, Pagès S, Punt PJ, Delattre M, Haon M, Van Den Hondel CAMJJ,
1143 Sigoillot JC, Lesage-Meessen L, Asther M (2003) Overproduction of the *Aspergillus niger* feruloyl
1144 esterase for pulp bleaching application. Appl Microbiol Biotechnol 62(4):349–355.
1145 <https://doi.org/10.1007/s00253-003-1325-4>

1146 Rozen S, Skaletsky H (2000) Primer3 on the WWW for general users and for biologist programmers.
1147 Methods in Molecular Biology (clifton, NJ) 132:365–386.

1148 Sakamoto T, Nishimura S, Kato T, Sunagawa Y, Tsuchiyama M, Kawasaki H (2005) Efficient
1149 extraction of ferulic acid from sugar beet pulp using the culture supernatant of *Penicillium chrysogenum*.
1150 J of Appl Glycosci 52(2):115–120. <https://doi.org/10.5458/jag.52.115>

1151 Schneider WDH, Goncalves TA, Uchima CA, Couger MB, Prade R, Squina FM, Dillon AJP, Camassola
1152 M (2016) *Penicillium echinulatum* secretome analysis reveals the fungi potential for degradation of
1153 lignocellulosic biomass. Biotechnol Biofuels 9:66. <https://doi.org/10.1186/s13068-016-0476-3>

1154 Sewalt V, Shanahan D, Gregg L, La Marta J, Carrillo R (2016) The generally recognized as safe (GRAS)
1155 process for industrial microbial enzymes. Ind Biotechnol 12(5):295–302.
1156 <https://doi.org/10.1089/ind.2016.0011>

1157 Song W, Han X, Qian Y, Liu G, Yao G, Zhong Y, Qu Y (2016) Proteomic analysis of the biomass
1158 hydrolytic potentials of *Penicillium oxalicum* lignocellulolytic enzyme system. Biotechnol Biofuels
1159 9(1):68–68. <https://doi.org/10.1186/s13068-016-0477-2>

1160 de Souza WR (2013) Microbial degradation of lignocellulosic biomass. In: Chandel A, da Silvia SS
1161 (eds). InTech, Rijeka, Croacia, pp 135–152.

1162 Stajich JE, Berbee ML, Blackwell M, Hibbett DS, James TY, Spatafora JW, Taylor JW (2009) The
1163 Fungi. Curr Biol 19(18):R840–R845. <https://doi.org/10.1016/j.cub.2009.07.004>

1164 Taofiq O, González-Paramás A, Barreiro M, Ferreira I (2017) Hydroxycinnamic acids and their
1165 derivatives: cosmeceutical significance, challenges and future perspectives, a review. Molecules
1166 22:281–281. <https://doi.org/10.3390/molecules22020281>

1167 Tatusov RL, Fedorova ND, Jackson JD, Jacobs AR, Kiryutin B, Koonin EV, Krylov DM, Mazumder R,
1168 Mekhedov SL, Nikolskaya AN, Rao BS, Smirnov S, Sverdlov AV, Vasudevan S, Wolf YI, Yin JJ,
1169 Natale DA (2003) The COG database: an updated version includes eukaryotes. *BMC Bioinformatics*
1170 4(1):41–41. <https://doi.org/10.1186/1471-2105-4-41>

1171 Terfehr D, Dahlmann TA, Kück U (2017) Transcriptome analysis of the two unrelated fungal β -lactam
1172 producers *Acremonium chrysogenum* and *Penicillium chrysogenum*: Velvet-regulated genes are major
1173 targets during conventional strain improvement programs. *BMC Genomics* 18(1):272–272.
1174 <https://doi.org/10.1186/s12864-017-3663-0>

1175 Terrasan CRF, Guisan JM, Carmona EC (2016) Xylanase and β -xylosidase from *Penicillium*
1176 *janczewskii*: Purification, characterization and hydrolysis of substrates. *Electron J Biotechnol* 23:54–62.
1177 <https://doi.org/10.1016/j.ejbt.2016.08.001>

1178 Thom C (1910) Cultural studies of species of *Penicillium*. *Bullet Bureau Animal Industry, USDA* 118:1–
1179 109.

1180 Tola M, Kebede B (2016) Occurrence, importance and control of mycotoxins: a review. *Cogent food*
1181 *agric* 2(1):1–12. <https://doi.org/10.1080/23311932.2016.1191103>

1182 Topakas E, Vafiadi C, Christakopoulos P (2007) Microbial production, characterization and applications
1183 of feruloyl esterases. *Process Biochem* 42:497–509. <https://doi.org/10.1016/j.procbio.2007.01.007>

1184 Tripathi N, Hills CD, Singh RS, Atkinson CJ (2019) Biomass waste utilisation in low-carbon products:
1185 harnessing a major potential resource. *npj Climate and Atmospheric Science* 2(1)
1186 <https://doi.org/10.1038/s41612-019-0093-5>

1187 Udatha DBRKG, Kouskoumvekaki I, Olsson L, Panagiotou G (2011) The interplay of descriptor-based
1188 computational analysis with pharmacophore modeling builds the basis for a novel classification scheme
1189 for feruloyl esterases. *Biotechnol Adv* 29(1):94–110. <https://doi.org/10.1016/j.biotechadv.2010.09.003>

1190 Udatha DBRKG, Mapelli V, Panagiotou G, Olsson L (2012) Common and distant structural
1191 characteristics of feruloyl esterase families from *Aspergillus oryzae*. *PLoS ONE* 7(6):e39473–e39473.
1192 <https://doi.org/10.1371/journal.pone.0039473>

1193 Ullán RV, Campoy S, Casqueiro J, Fernández FJ, Martín JF (2007) Deacetylcephalosporin C production
1194 in *Penicillium chrysogenum* by expression of the isopenicillin N epimerization, ring expansion, and
1195 acetylation genes. *Chem Biol* 14:329–339. <https://doi.org/10.1016/j.chembiol.2007.01.012>

1196 van den Brink J, de Vries RP (2011) Fungal enzyme sets for plant polysaccharide degradation. *Appl*
1197 *Microbiol Biotechnol* 91(6):1477–1492. <https://doi.org/10.1007/s00253-011-3473-2>

1198 van den Berg MA, Albang R, Albermann K, Badger JH, Daran JM, Driessen MAJ, Garcia-Estrada C,
1199 Fedorova ND, Harris DM, Heijne WHM, Joardar V, Kiel WJAK, Kovalchuk A, Martín JF, Nierman
1200 WC, Nijland JG, Pronk JT, Roubos JA, van der Klei IJ, van Peij NNME, Veenhuis M, Döhren H,

1201 Wagner C, Wortman J, Bovenberg RAL (2008) Genome sequencing and analysis of the filamentous
1202 fungus *Penicillium chrysogenum*. Nat Biotechnol 26(10):1161–1168. <https://doi.org/10.1038/nbt.1498>

1203 van Egmond HP, Schothorst RC, Jonker MA (2007) Regulations relating to mycotoxins in food. Anal
1204 Bioanal Chem 389(1):147–157. <https://doi.org/10.1007/s00216-007-1317-9>

1205 Vasco-Cárdenas MF, Baños S, Ramos A, Martín JF, Barreiro C (2013) Proteome response of
1206 *Corynebacterium glutamicum* to high concentration of industrially relevant C4 and C5 dicarboxylic
1207 acids. J Proteomics 85:65–88. <https://doi.org/10.1016/j.jprot.2013.04.019>

1208 Ventola CL (2015) The antibiotic resistance crisis: part 1: causes and threats. P & T : a Peer-Reviewed
1209 Journal for Formulary Management 40(4):277–283.

1210 Vila-Donat P, Marín S, Sanchis V, Ramos AJ (2018) A review of the mycotoxin adsorbing agents, with
1211 an emphasis on their multibinding capacity, for animal feed decontamination. Food Chem Toxicol
1212 114:246–259. <https://doi.org/10.1016/j.fct.2018.02.044>

1213 Visagie CM, Houbraken J, Frisvad JC, Hong SB, Klaassen CHW, Perrone G, Seifert KA, Varga J,
1214 Yaguchi T, Samson RA (2014) Identification and nomenclature of the genus *Penicillium*. Stud Mycol
1215 78(1):343–371. <https://doi.org/10.1016/j.simyco.2014.09.001>

1216 Wagacha JM, Muthomi JW (2008) Mycotoxin problem in Africa: current status, implications to food
1217 safety and health and possible management strategies. Int J Food Microbiol 124(1):1–12.
1218 <https://doi.org/10.1016/j.ijfoodmicro.2008.01.008>

1219 Wang L, Li Z, Zhu M, Meng L, Wang H, Ng TB (2016a) An acidic feruloyl esterase from the mushroom
1220 *Lactarius hatsudake*: a potential animal feed supplement. Int J Biol Macromol 93:290–295.
1221 <https://doi.org/10.1016/j.ijbiomac.2016.08.028>

1222 Wang M, Carver JJ, Phelan VV, Sanchez LM, Garg N, Peng Y, Nguyen DD, Watrous J, Kaponi CA,
1223 Luzzatto-Knaan T, Porto C, Bouslimani A, Melnik AV, Meehan MJ, Liu WT, Crüsemann M, Boudreau
1224 PD, Esquenazi E, Sandoval-Calderón M, Kersten RD, Pace LA, Quinn RA, Duncan KR, Hsu CC, Floros
1225 DJ, Gavilan RG, Kleigrew K, Northen T, Dutton RJ, Parrot D, Carlson EE, Aigle B, Michelsen CF,
1226 Jelsbak L, Sohlenkamp C, Pevzner P, Edlund A, McLean J, Piel J, Murphy BT, Gerwick L, Liaw CC,
1227 Yang YL, Humpf HU, Maansson M, Keyzers RA, Sims AC, Johnson AR, Sidebottom AM, Sedio BE,
1228 Klitgaard A, Larson CB, Boya CAP, Torres-Mendoza D, Gonzalez DJ, Silva DB, Marques LM,
1229 Demarque DP, Pociute E, O’Neill EC, Briand E, Helfrich EJN, Granatosky EA, Glukhov E, Ryffel F,
1230 Houson H, Mohimani H, Kharbush JJ, Zeng Y, Vorholt JA, Kurita KL, Charusanti P, McPhail KL,
1231 Nielsen KF, Vuong L, Elfeki M, Traxler MF, Engene N, Koyama N, Vining OB, Baric R, Silva RR,
1232 Mascuch SJ, Tomasi S, Jenkins S, Macherla V, Hoffman T, Agarwal V, Williams PG, Dai J, Neupane
1233 R, Gurr J, Rodríguez AMC, Lamsa A, Zhang C, Dorrestein K, Duggan BM, Almaliti J, Allard PM,
1234 Phapale P, Nothias LF, Alexandrov T, Litaudon M, Wolfender JL, Kyle JE, Metz TO, Peryea T, Nguyen
1235 DT, VanLeer D, Shinn P, Jadhav A, Müller R, Waters KM, Shi W, Liu X, Zhang L, Knight R, Jensen

1236 PR, Pálsson B, Pogliano K, Linington RG, Gutiérrez M, Lopes NP, Gerwick WH, Moore BS, Dorrestein
1237 PC, Bandeira N (2016b) Sharing and community curation of mass spectrometry data with Global Natural
1238 Products Social Molecular Networking. *Nat Biotechnol* 34(8):828–837.
1239 <https://doi.org/10.1038/nbt.3597>

1240 Ward OP (2012) Production of recombinant proteins by filamentous fungi. *Biotechnol Adv* 30(5):1119–
1241 1139. <https://doi.org/10.1016/j.biotechadv.2011.09.012>

1242 Wei H, Xu Q, Taylor LE, Baker JO, Tucker MP, Ding S-Y (2009) Natural paradigms of plant cell wall
1243 degradation. *Curr Opin Biotechnol* 20(3):330–338. <https://doi.org/10.1016/j.copbio.2009.05.008>

1244 Wingfield P (1998) Protein precipitation using ammonium sulfate. John Wiley & Sons, Inc., Hoboken,
1245 New Jersey, United States, pp A.3F.1–A.3F.8.

1246 Xiao Z, Storms R, Tsang A (2005) Microplate-based carboxymethylcellulose assay for endoglucanase
1247 activity. *Anal Biochem* 342(1):176–178. <https://doi.org/10.1016/j.ab.2005.01.052>

1248 Zhang SB, Zhai HC, Wang L, Yu GH (2013) Expression, purification and characterization of a feruloyl
1249 esterase A from *Aspergillus flavus*. *Protein Expression Purif* 92(1):36–40.
1250 <https://doi.org/10.1016/j.pep.2013.08.009>

1251 Zhao W, Li C, Liang J, Sun S (2014) The *Aspergillus fumigatus* β -1,3-glucanosyltransferase Gel7 plays
1252 a compensatory role in maintaining cell wall integrity under stress conditions. *Glycobiology* 24(5):418–
1253 427. <https://doi.org/10.1093/glycob/cwu003>

1254 Zhu Z-J, Schultz AW, Wang J, Johnson CH, Yannone SM, Patti GJ, Siuzdak G (2013) Liquid
1255 chromatography quadrupole time-of-flight mass spectrometry characterization of metabolites guided by
1256 the METLIN database. *Nat Protoc* 8(3):451–460. <https://doi.org/10.1038/nprot.2013.004>

1257 Zuin VG, Ramin LZ (2018) Green and sustainable separation of natural products from agro-industrial
1258 waste: challenges, potentialities, and perspectives on emerging approaches. *Top Curr Chem* 376(1):3–
1259 3. <https://doi.org/10.1007/s41061-017-0182-z>

1260 Zwane EN, Rose SH, van Zyl WH, Rumbold K, Viljoen-Bloom M (2014) Overexpression of *Aspergillus*
1261 *tubingensis* *faeA* in protease-deficient *Aspergillus niger* enables ferulic acid production from plant
1262 material. *J Ind Microbiol Biotechnol* 41(6):1027–1034. <https://doi.org/10.1007/s10295-014-1430-7>
1263

Table 1. List of oligonucleotides used in this work. Their sequence and applications are indicated. Target sequences for relevant restriction sites appear underlined.

Primer	Sequence (5' → 3') and features	Application
<i>faeA</i> -F	GGA <u>AGATCT</u> ATGAAAATCTCCGCACCACG (<i>Bgl</i> III site)	Construction of p <i>SfaeA</i> plasmid
<i>faeA</i> -R	AAA <u>AGGCTCT</u> ACCAGCTGCAAGCTCCGC (<i>Stu</i> I site)	Construction of p <i>SfaeA</i> plasmid
<i>faeB</i> -F	GGA <u>AGATCT</u> ATGACTCGTCTTCATGTGTT (<i>Bgl</i> III site)	Construction of p <i>SfaeB</i> plasmid
<i>faeB</i> -R	AAA <u>AGGCTCT</u> TAAACACACTGCCAAGCGT (<i>Stu</i> I site)	Construction of p <i>SfaeB</i> plasmid
<i>Pgdh</i> -F	GGACTCCCTAATGGATTCCGA	Creation of specific probes from <i>faeA/faeB</i> genes, used in RT-qPCR
<i>Tcyc</i> -R	GAAAAGGGGGACGGATCTCCG	Used together with <i>Pgdh</i> -F for the same purposes
<i>actA</i> -F	CTGGCCGTGATCTGACCGACTAC	Creation of <i>actA</i> specific probe from <i>actA</i> constitutive gene, used in RT-qPCR
<i>actA</i> -R	GGGGGAGCGATCTTGACCT	Used together with <i>actA</i> -F for the same purposes
1- <i>faeB</i> -F	CTTCATGTGTTGCCCTTGTT	Clone sequencing and verification
2- <i>faeB</i> -F	TTCCCGAAACCAACAT	Clone sequencing and verification
3- <i>faeB</i> -F	CGCTGGTGCCCTGCTATC	Clone sequencing and verification
4- <i>faeB</i> -F	ATCCTCGCTGCACCAATAAT	Clone sequencing and verification
5- <i>faeB</i> -F	ATTGCGGTGATGGAGATG	Clone sequencing and verification
1- <i>faeB</i> -R	CACACTGCCAAGCGTTCT	Clone sequencing and verification
2- <i>faeB</i> -R	CAGCTTGAGTTGTGCG	Clone sequencing and verification
3- <i>faeB</i> -R	GACTTGGGCGCTTGTGAGAC	Clone sequencing and verification
4- <i>faeB</i> -R	TTGTCGAAGCCCTCCTCA	Clone sequencing and verification
5- <i>faeB</i> -R	CGTGATCTCGCTGCTA	Clone sequencing and verification

Table 2. Protein spots identified by mass spectrometry (MALDI TOF/TOF). Mowse score from Mascot search (protein score), protein coverage (%), secretion parameters [classical secretion systems: SignalP and score; nonclassical systems: SecretomeP and score] are indicated. COG functional categories [C: energy production and conversion; E: amino acid transport and metabolism; G: carbohydrate metabolism and transport; I: lipid transport and metabolism; J: translation, ribosomal structure, and biogenesis; M: cell wall/membrane/envelope biogenesis; P: inorganic ion transport and metabolism; Q: secondary metabolites biosynthesis, transport, and catabolism; S: function unknown], EC numbers, CAZy families and enzyme descriptions are also included. [N/A, not applicable].

Spot no	Protein name	Description	Protein score	Coverage (%)	SignalP	Likelihood (SignalP)	SecretomeP	NN-score (SecretomeP)	Functional category (COG)
1	Pc21g23210	Pc21g23210 protein (glycoside hydrolase family 16, CRH1, predicted)	428	34	Yes	0.9964	—	—	G, M
2	Pc18g01940	β -glucosidase	311	27	Yes	0.9637	—	—	G
3	Pc18g01940	β -glucosidase	605	35	Yes	0.9637	—	—	G
4	Pc12g11110	β -glucosidase	151	17	Yes	0.9768	—	—	G
5	Pc22g14710	Pc22g14710 protein (O-glucosyl hydrolase; xylan 1,4- β -xylosidase activity; glycoside hydrolase family 3)	181	21	Yes	0.967	—	—	G
6	Pc22g14710	Pc22g14710 protein (O-glucosyl hydrolase; xylan 1,4- β -xylosidase activity; glycoside hydrolase family 3)	128	26	Yes	0.967	—	—	G
6	Pc22g24800	β -N-acetylhexosaminidase	112	17	Yes	0.9954	—	—	G
7	Pc22g24800	β -N-acetylhexosaminidase	127	24	Yes	0.9954	—	—	G
8	Pc22g24800	β -N-acetylhexosaminidase	184	27	Yes	0.9954	—	—	G
9	Pc22g24800	β -N-acetylhexosaminidase	660	36	Yes	0.9954	—	—	G
10	Pc16g03030	Pc + G13:G1416g03030 protein (saponin hydrolase)	296	25	Yes	0.82	—	—	S
11	Pc16g03030	Pc16g03030 protein (saponin hydrolase)	281	38	Yes	0.82	—	—	S
12	Pc20g10170	Pc20g10170 protein (β -glucosidase; glycoside hydrolase family 3)	351	28	Yes	0.9782	—	—	G
13	Pc20g10170	Pc20g10170 protein (β -glucosidase; glycoside hydrolase family 3)	664	28	Yes	0.9782	—	—	G
14	Pc16g11860	Catalase	178	24	Yes	0.9604	—	—	C, P, Q
15	Pc16g11860	Catalase	486	44	Yes	0.9604	—	—	C, P, Q
16	Pc16g11860	Catalase	349	30	Yes	0.9604	—	—	C, P, Q
17	Pc16g11860	Catalase	657	41	Yes	0.9604	—	—	C, P, Q
18	Pc16g11860	Catalase	886	49	Yes	0.9604	—	—	C, P, Q
19	Pc16g11860	Catalase	335	34	Yes	0.9604	—	—	C, P, Q
20	Pc16g11860	Catalase	575	39	Yes	0.9604	—	—	C, P, Q
21	Pc20g02640	Pc20g02640 protein (glutaminase)	265	29	Yes	0.9841	—	—	S
22	Pc16g11860	Catalase	787	46	Yes	0.9604	—	—	C, P, Q
23	Pc20g02640	Pc20g02640 protein (glutaminase)	306	29	Yes	0.9841	—	—	S
24	Pc20g02640	Pc20g02640 protein (glutaminase)	244	26	Yes	0.9841	—	—	S
25	Pc20g02640	Pc20g02640 protein (glutaminase)	202	26	Yes	0.9841	—	—	S
26	EN45_021350	β -galactosidase	230	15	Yes	0.8834	—	—	G
26	Pc20g02640	Pc20g02640 protein (glutaminase)	191	26	Yes	0.9841	—	—	S
27	Pc16g11860	Catalase	1090	51	Yes	0.9604	—	—	C, P, Q
28	Pc22g24800	β -N-acetylhexosaminidase	350	26	Yes	0.9954	—	—	G
29	Pc20g02640	Pc20g02640 protein (glutaminase)	794	42	Yes	0.9841	—	—	S

Table 2 (continued)

Spot no	Protein name	Description	Protein score	Coverage (%)	SignalP	Likelihood (SignalP)	SecretomeP	NN-score (SecretomeP)	Functional category (COG)
30	Pc22g08520	Pc22g08520 protein (β -glucuronidase; glycoside hydrolase family 79)	133	22	Yes	0.9896	—	—	S
31	Pc20g02640	Pc20g02640 protein (glutaminase)	568	32	Yes	0.9841	—	—	S
32	Pc22g08520	Pc22g08520 protein (β -glucuronidase; glycoside hydrolase family 79)	495	29	Yes	0.9896	—	—	S
33	Pc13g15360	Carboxylic ester hydrolase	138	20	Yes	0.9458	—	—	G, I
34	Pc12g08730	Pc12g08730 protein (β -N-acetylglucosaminidase, glycoside hydrolase family 84)	562	32	Yes	0.9976	—	—	J, O
35	Pc16g08980	Endo-1,3(4)- β -glucanase	416	42	Yes	0.9603	—	—	G, M
36	Pc16g11860	Catalase	352	27	Yes	0.9604	—	—	C, P, Q
37	Pc22g01750	Pc22g01750 protein (amidase)	99	27	No	0.0007	No	0.531	J
38	Pc20g01970	Glucanase	226	38	Yes	0.9925	—	—	G
39	Pc12g08300	Carboxylic ester hydrolase	261	24	Yes	0.9953	—	—	G
40	Pc20g01970	Glucanase	479	42	Yes	0.9925	—	—	G
41	Pc12g08300	Carboxylic ester hydrolase	494	30	Yes	0.9953	—	—	G
42	Pc12g08300	Carboxylic ester hydrolase	734	43	Yes	0.9953	—	—	G
43	Pc22g08520	Pc22g08520 protein (β -glucuronidase; glycoside hydrolase family 79)	413	22	Yes	0.9896	—	—	S
43	Pc20g10360	β -N-acetylhexosaminidase hex	260	30	Yes	0.978	—	—	G
44	Pc12g08300	Carboxylic ester hydrolase	744	37	Yes	0.9953	—	—	G
45	Pc20g10360	β -N-acetylhexosaminidase hex	426	46	Yes	0.978	—	—	G
46	Pc20g10360	β -N-acetylhexosaminidase hex	438	42	Yes	0.978	—	—	G
47	Pc20g10360	β -N-acetylhexosaminidase hex	472	35	Yes	0.978	—	—	G
48	Pc20g10360	β -N-acetylhexosaminidase hex	446	48	Yes	0.978	—	—	G
49	Pc20g10360	β -N-acetylhexosaminidase hex	270	30	Yes	0.978	—	—	G
50	Pc20g01970	Glucanase	513	43	Yes	0.9925	—	—	G
51	Pc20g10360	β -N-acetylhexosaminidase hex	278	25	Yes	0.978	—	—	G
52	Pc20g10360	β -N-acetylhexosaminidase hex	279	25	Yes	0.978	—	—	G
53	Pc20g10360	β -N-acetylhexosaminidase hex	242	28	Yes	0.978	—	—	G
54	Pc20g10360	β -N-acetylhexosaminidase hex	412	42	Yes	0.978	—	—	G
55	Pc20g10360	β -N-acetylhexosaminidase hex	520	42	Yes	0.978	—	—	G
56	Pc20g10360	β -N-acetylhexosaminidase hex	463	42	Yes	0.978	—	—	G
57	Pc20g10360	β -N-acetylhexosaminidase hex	361	30	Yes	0.978	—	—	G

Table 2 (continued)

Spot no	Protein name	Description	Protein score	Coverage (%)	SignalP	Likelihood (SignalP)	SecretomeP	NN-score (SecretomeP)	Functional category (COG)
58	Pc20g10360	β -N-acetylhexosaminidase hex	375	37	Yes	0.978	—	—	G
59	Pc20g01970	Glucanase	245	40	Yes	0.9925	—	—	G
60	Pc20g10360	β -N-acetylhexosaminidase hex	759	46	Yes	0.978	—	—	G
61	Pc20g10360	β -N-acetylhexosaminidase hex	706	46	Yes	0.978	—	—	G
62	Pc20g10360	β -N-acetylhexosaminidase hex	957	44	Yes	0.978	—	—	G
63	Pc21g14410	Pc21g14410 protein (endoglucanase; glycoside hydrolase family 5)	271	34	Yes	0.9964	—	—	G
64	Pc22g19620	α -L-arabinofuranosidase	173	35	Yes	0.9955	—	—	G, M
65	Pc14g00370	Rhamnogalacturonate lyase	504	40	Yes	0.9952	—	—	G, M
66	Pc14g00370	Rhamnogalacturonate lyase	217	35	Yes	0.9952	—	—	G, M
67	Pc18g05490	Glucanase	159	33	Yes	0.9873	—	—	G
68	Pc18g05490	Glucanase	167	30	Yes	0.9873	—	—	G
69	Pc18g05490	Glucanase	176	30	Yes	0.9873	—	—	G
70	Pc18g05490	Glucanase	84	27	Yes	0.9873	—	—	G
71	Pc12g14860	Extracellular acid phosphatase PhoA	253	39	Yes	0.96	—	—	O, S
72	Pc22g19620	α -L-arabinofuranosidase	95	28	Yes	0.9955	—	—	G, M
73	Pc21g12590	FAD-linked oxidoreductase chyH	284	36	Yes	0.9255	—	—	C
74	Pc22g19620	α -L-arabinofuranosidase	318	35	Yes	0.9955	—	—	G, M
75	Pc22g19620	α -L-arabinofuranosidase	701	40	Yes	0.9955	—	—	G, M
76	Pc21g12590	FAD-linked oxidoreductase chyH	391	27	Yes	0.9255	—	—	C
77	Pc22g19620	α -L-arabinofuranosidase	102	29	Yes	0.9955	—	—	G, M
78	Pc14g00370	Rhamnogalacturonate lyase	666	50	Yes	0.9952	—	—	G, M
79	EN45_000350	Rhamnogalacturonate lyase	911	54	Yes	0.9952	—	—	G, S
80	Pc22g19620	α -L-arabinofuranosidase	331	35	Yes	0.9955	—	—	G, M
81	Pc22g19620	α -L-arabinofuranosidase	754	42	Yes	0.9955	—	—	G, M
82	Pc20g10360	β -N-acetylhexosaminidase hex	263	29	Yes	0.978	—	—	G
83	Pc21g12590	FAD-linked oxidoreductase chyH	543	37	Yes	0.9255	—	—	C
84	Pc22g01850	1,4- α -D-glucan glucohydrolase	469	53	Yes	0.8674	—	—	G
85	Pc16g14170	α -1,2-mannosidase	260	47	Yes	0.9931	—	—	G
86	Pc22g22810	Pc22g22810 protein (putative thioredoxin reductase)	207	43	Yes	0.9456	—	—	C, O
87	Pc21g19010	Pc21g19010 protein (metal-independent α -mannosidase; glycoside hydrolase family 125)	89	24	Yes	0.9869	—	—	G, S
88	Pc21g23210	Pc21g23210 protein (glycosidase; glycoside hydrolase family 16)	178	29	Yes	0.9964	—	—	G, M
89	Pc21g23210	Pc21g23210 protein (glycosidase; glycoside hydrolase family 16)	542	56	Yes	0.9964	—	—	G, M

Table 2 (continued)

Spot no	Protein name	Description	Protein score	Coverage (%)	SignalP	Likelihood (SignalP)	SecretomeP	NN-score (SecretomeP)	Functional category (COG)
90	Pc21g23210	Pc21g23210 protein (glycosidase; glycoside hydrolase family 16)	147	23	Yes	0.9964	—	—	G, M
91	Pc18g05530	Pc18g05530 protein (FAD-linked oxidoreductase)	184	22	Yes	0.896	—	—	C
92	Pc21g19010	Pc21g19010 protein (metal-independent α -mannosidase; glycoside hydrolase family 125)	349	28	Yes	0.9869	—	—	G, S
93	Pc13g09520	Chitinase	86	33	No	0.0039	No	0.586	G
94	Pc13g09520	Chitinase	237	48	No	0.0039	No	0.586	G
95	Pc22g00820	Beta-xylanase	117	20	Yes	0.9637	—	—	G
96	Pc18g01880	Exo-arabinanase abnx	190	24	Yes	0.7453	—	—	G, S, O
97	Pc18g01880	Exo-arabinanase abnx	228	24	Yes	0.7453	—	—	G, S, O
98	Pc18g01880	Exo-arabinanase abnx	225	24	Yes	0.7453	—	—	G, S, O
99	Pc21g19010	Pc21g19010 protein (metal-independent α -mannosidase; glycoside hydrolase family 125)	278	24	Yes	0.9869	—	—	G, S
100	Pc18g01880	Exo-arabinanase abnx	658	40	Yes	0.7453	—	—	G, S, O
101	Pc18g01880	Exo-arabinanase abnx	148	24	Yes	0.7453	—	—	G, S, O
102	Pc18g01880	Exo-arabinanase abnx	260	28	Yes	0.7453	—	—	G, S, O
103	Pc18g01880	Exo-arabinanase abnx	643	41	Yes	0.7453	—	—	G, S, O
104	EN45_103640	Chitinase	150	31	Yes	0.9956	—	—	G
105	EN45_103640	Chitinase	405	62	Yes	0.9956	—	—	G
106	EN45_103640	Chitinase	554	80	Yes	0.9956	—	—	G
107	Pc18g03120	Pc18g03120 protein (β -1,3-glucanase; glycoside hydrolase family 64)	283	45	No	0.0024	Yes	0.72	S
108	Pc22g15910	Probable Xaa-Pro aminopeptidase P	105	15	No	0.0017	No	0.434	E
109	Pc13g09680	Penicillopepsin (aspartic-type endopeptidase activity)	140	32	Yes	0.975	—	—	M, O
110	Pc21g09850	Pc21g09850 protein (pectin lyase; polysaccharide lyase 1)	363	47	Yes	0.9005	—	—	G
111	Pc22g24890	Pc22g24890 protein (pectate lyase; polysaccharide lyase family 1)	219	49	Yes	0.989	—	—	G
112	Pc22g24890	Pc22g24890 protein (pectate lyase; polysaccharide lyase family 1)	573	50	Yes	0.989	—	—	G
113	Pc22g24890	Pc22g24890 protein (pectate lyase; polysaccharide lyase family 1)	876	52	Yes	0.989	—	—	G
114	Pc13g08730	Endo-1,3-beta-glucanase egIC	140	46	Yes	0.9941	—	—	G
115	Pc21g14160	Alkaline serine protease AAM33821	182	43	Yes	0.924	—	—	O
116	Pc13g08730	Endo-1,3-beta-glucanase egIC	333	73	Yes	0.9941	—	—	G
117	Pc21g23210	Pc21g23210 protein (glycosidase; glycoside hydrolase family 16)	146	44	Yes	0.9964	—	—	G, M

Table 2 (continued)

Spot no	Protein name	Description	Protein score	Coverage (%)	SignalP	Likelihood (SignalP)	SecretomeP	NN-score (SecretomeP)	Functional category (COG)
118	Pc21g23210	Pc21g23210 protein (glycosidase; glycoside hydrolase family 16)	142	33	Yes	0.9964	—	—	G, M
119	Pc21g23210	Pc21g23210 protein (glycosidase; glycoside hydrolase family 16)	184	40	Yes	0.9964	—	—	G, M
120	Pc20g09400	Pc20g09400 protein (serine-type peptidase activity; peptidase family S9)	174	17	No	0.0041	Yes	0.682	E, O
120	Pc22g13950	Pc22g13950 protein (aminopeptidase; peptidase family M18)	168	25	No	0.0063	No	0.532	E

Table 3. Cellulase and xylanolytic activities of *P. rubens* B13. Reactions performed at pH 5.0 and 50 °C. U, unit, defined as the amount of enzyme that releases one μ mole of product (4-nitrophenol for cellobiohydrolase, β -glucosidase, and β -xylosidase; glucose for endoglucanase; xylose for endoxylanase) per min at the given conditions. Values given as means, including standard deviations.

Lignocellulolytic activity	Specific activity (U/mg total protein)
β -glucosidase	2.65 ± 0.27
Cellobiohydrolase	0.52 ± 0.03
Endoglucanase	0.33 ± 0.039
β -xylosidase	0.33 ± 0.02
Endoxylanase	0.3 ± 0.03

Table 4. Simple sugars released after treatment of sugar beet pulp (SBP) with enzyme extracts recovered from *P. rubens* Wisconsin 54–1255 (WIS) and transformant B13 (B13) fermentations on M-SBP. Reactions performed adding 15 mg extract/g SBP, 24 h at pH 5.0, 50 °C and 175 rpm. Values given as means from three replicates, including the standard deviations.

Monosaccharide/ disaccharide	Saccharification power (g/L released) by WIS	Saccharification power (g/L released) by B13
Glucose	2.72 ± 0.41	3.35 ± 0.99
Galactose	N/D ^a	N/D ^a
Fructose	1.88 ± 0.20	2.08 ± 0.67
Arabinose	3.62 ± 0.82	3.83 ± 0.68
Sucrose	N/D ^a	N/D ^a

^a N/D, non-detected

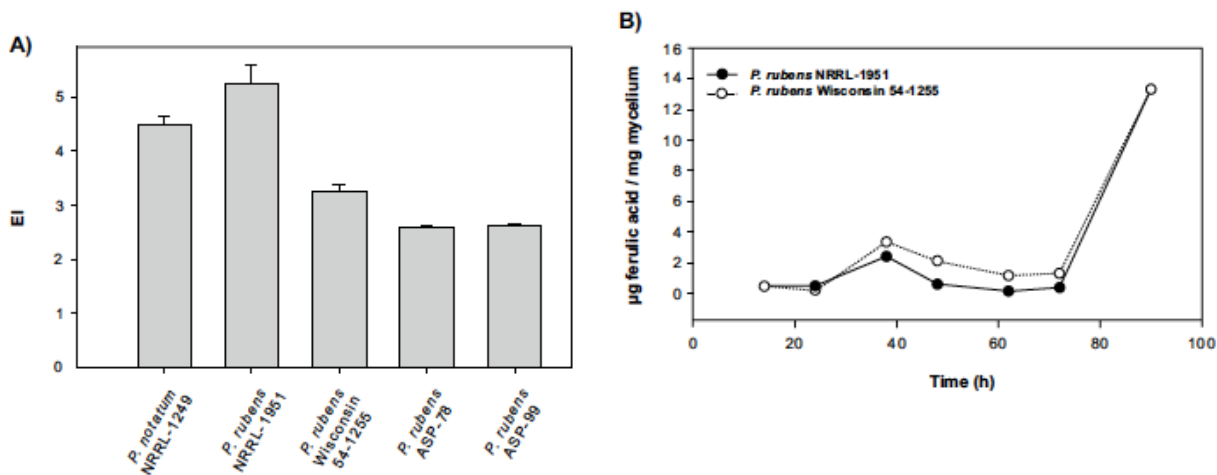


Fig. 1. A Enzymatic indices (EI) for each analyzed strain (indirect measurement of FAE activity through the ability to hydrolyze ethyl ferulate on a plate assay; $[EI = (\text{diameter of the colony} + \text{diameter of the degradation halo}) / \text{diameter of the colony}]$). Strain names are indicated in the figure. **B** FAE activity of *P. rubens* Wisconsin 54–1255 and *P. rubens* NRRL-1951, determined by the release of ferulic acid from sugar beet pulp in liquid medium at 28 °C and 250 rpm.

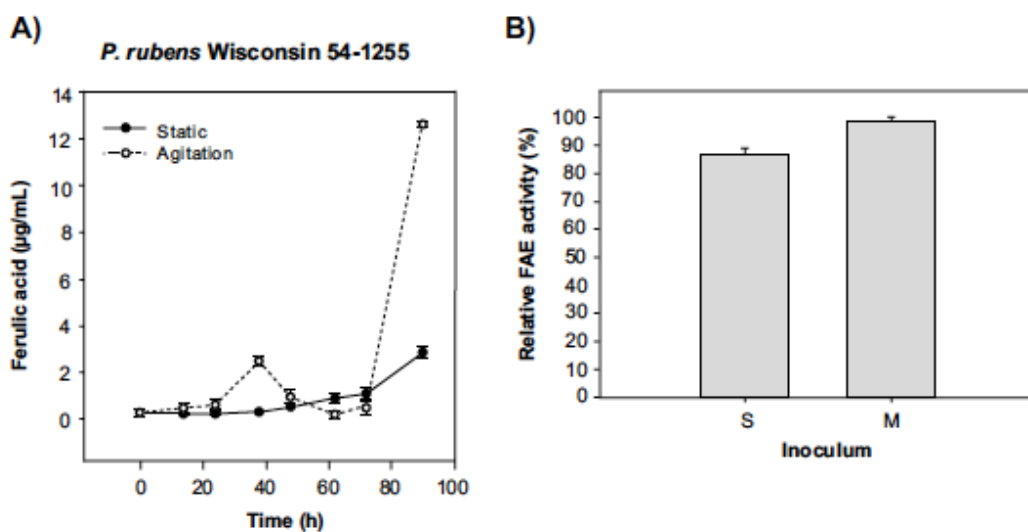


Fig. 2. A Comparative analysis of *P. rubens* Wisconsin 54–1255 FAE activity in submerged culture at 28 °C, with (250 rpm) or without constant agitation, through the release of ferulic acid from sugar beet pulp. **B** FAE activity of enzyme extracts obtained from *P. rubens* Wisconsin 54–1255 grown in M-SBP medium, after being inoculated with a spore suspension (S) or 10% (v/v) of a seed culture grown for 24 h in PMMY medium, at 28 °C and 250 rpm (M). Data expressed as relative FAE activity values compared to the maximum (100%).

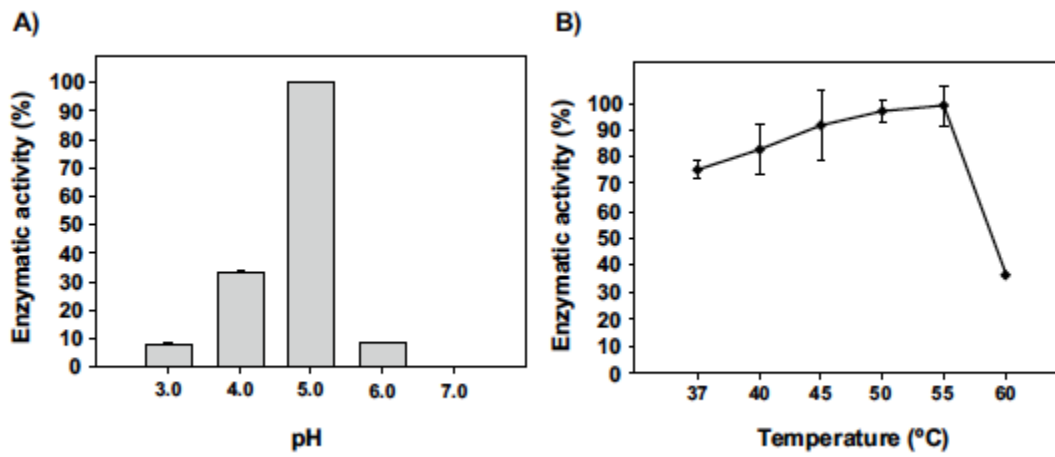


Fig. 3. Effect of pH and temperature on FAE activity of *P. rubens* Wisconsin 54-1255 enzyme extract against methyl ferulate. FAE activity is expressed as relative values compared to the maximum (100%). **A** Influence of pH on FAE activity at 37 °C. **B** Influence of temperature.

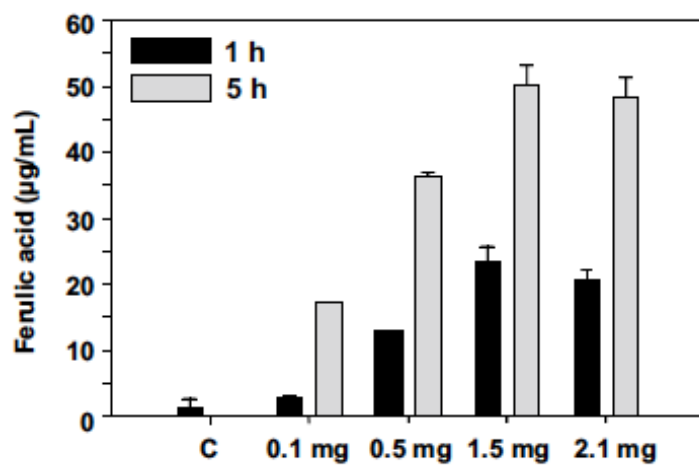


Fig. 4. Release of ferulic acid from sugar beet pulp at pH 5.0, 50 °C, and 175 rpm, by different concentrations of *P. rubens* Wisconsin 54-1255 enzyme extract and at two incubation times (1 h and 5 h). C, control without enzyme extract.

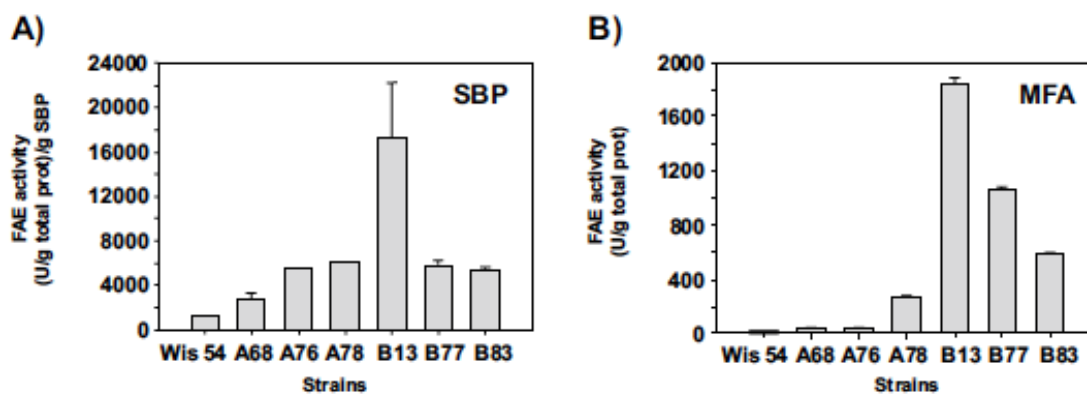


Fig. 5. FAE activity of *P. rubens* Wisconsin 54–1255 and its transformants A68, A76, A78, B13, B77, and B83 enzyme extracts against the substrates sugar beet pulp (SBP) (A) and methyl ferulate (B). One unit (U) corresponds to the amount of enzyme that releases one μmol of ferulic acid per min under the assay conditions (pH 5.0 and 50 °C).

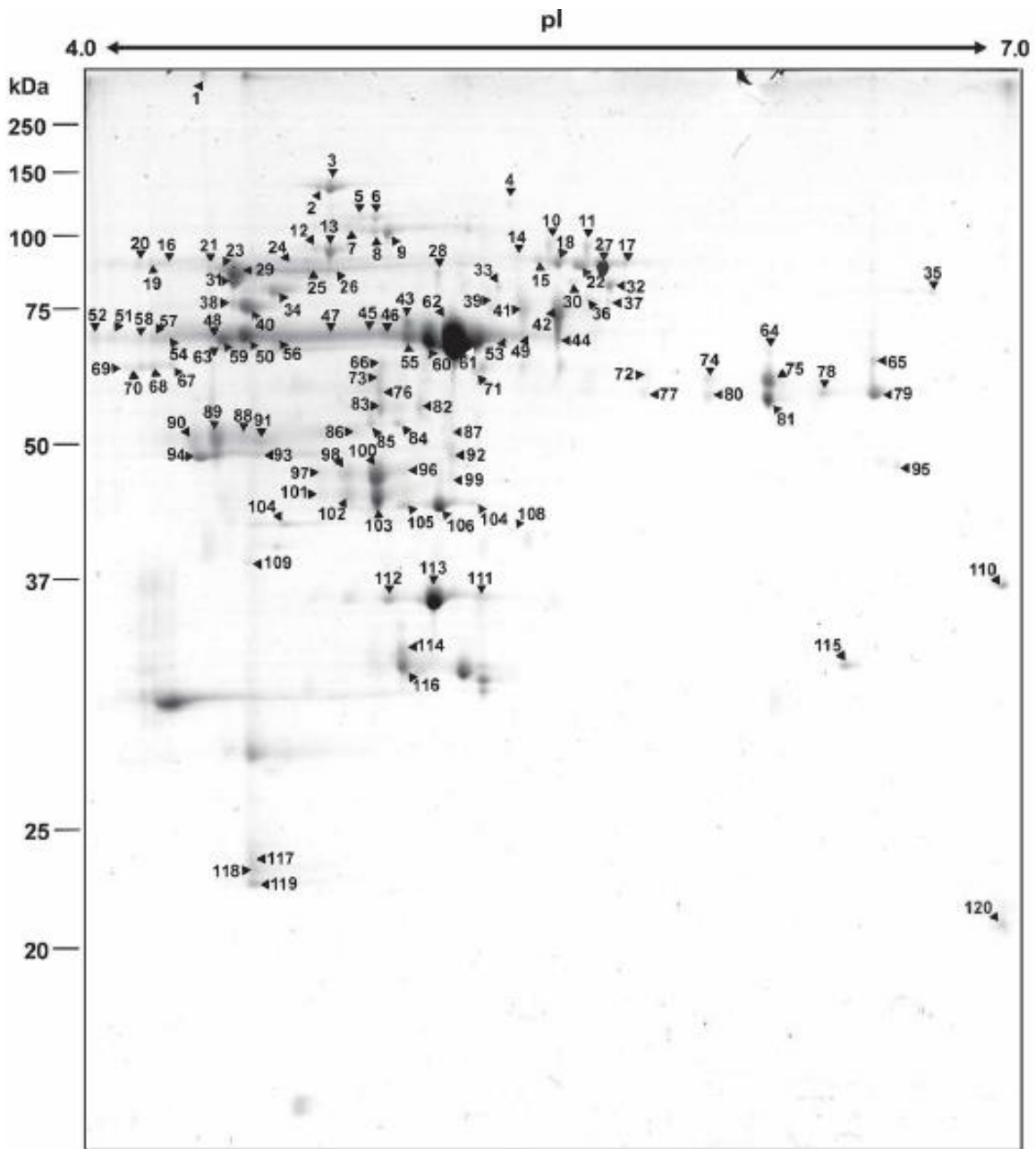


Fig. 6. Reference map of the *P. rubens* B13 grown in M-SBP partial extracellular proteome; 205 protein spots were visualized in a 4.0–7.0 pH range, and 120 were successfully identified (numbered in the gel image. Numbers correspond to those in Table 2 and Supplementary File S7). The pH range is marked above the gel and molecular weights (kDa), on the left.

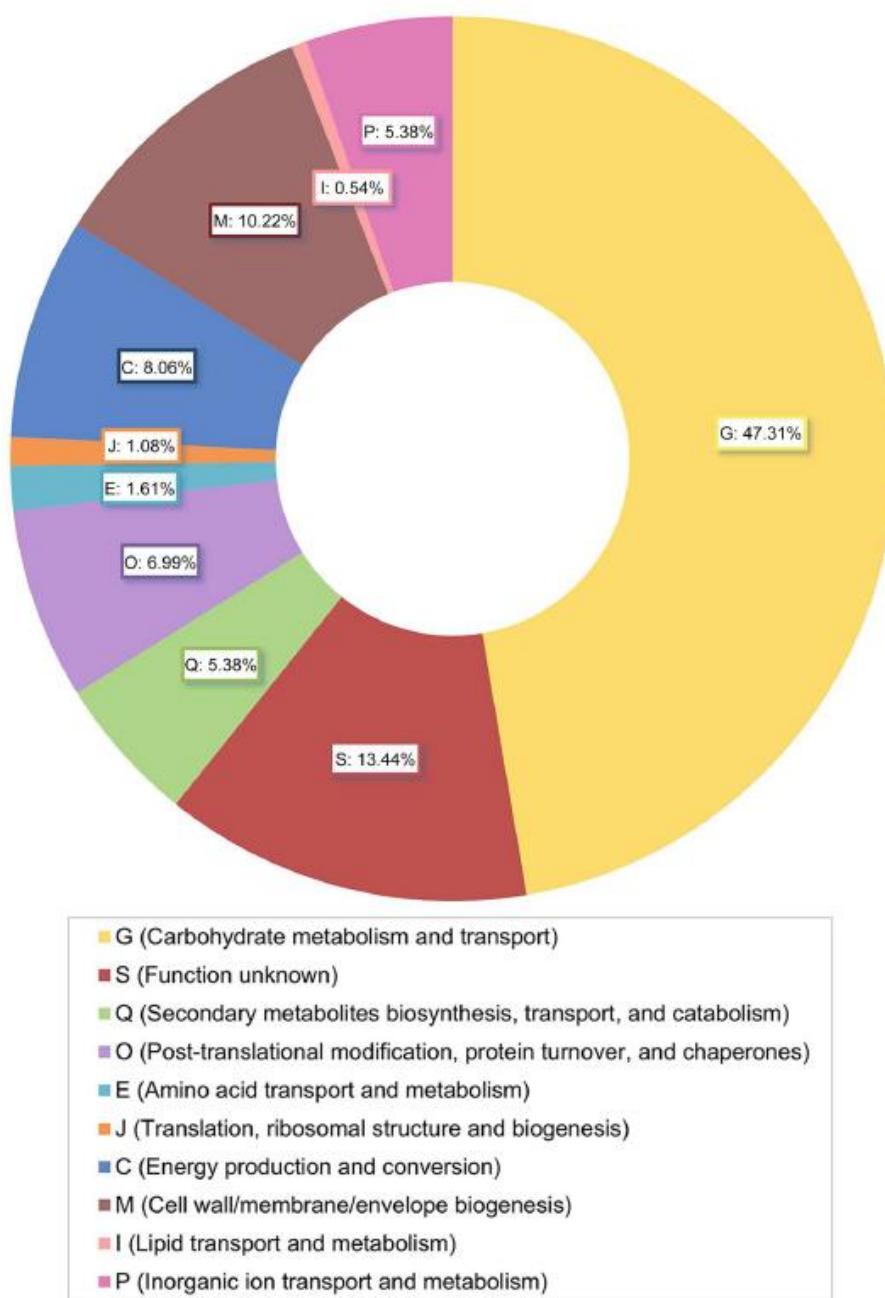


Fig. 7. Functional classification of all the protein species identified from *P. rubens* B13 partial extracellular proteomes when grown on the lignocellulosic natural substrate sugar beet pulp. The classification was based on a functional annotation according to the COG (Clusters of Orthologous Groups of proteins) system, which includes eukaryote organisms (KOG), via the eggNOG 5.0 online orthology resource (Huerta- Cepas et al. 2019; Tatusov et al. 2003).

***Penicillium chrysogenum* as a profitable fungal factory for feruloyl esterases**

Laura García-Calvo ^{1,a} §; Raquel Rodríguez-Castro ¹ §; Ricardo V. Ullán ^{1,b} *; Silvia M. Albillos ²; Marta Fernández-Aguado ¹; Cláudia M. Vicente ^{1,c}; Kristin F. Degnes ³; Håvard Sletta ³; Carlos Barreiro ⁴ *

¹ INBIOTEC (Instituto de Biotecnología de León). Avda. Real 1 - Parque Científico de León 24006, León, Spain.

² Área de Bioquímica y Biología Molecular, Departamento de Biotecnología y Ciencia de los Alimentos, Facultad de Ciencias, Universidad de Burgos, 09001 Burgos, Spain.

³ SINTEF Industry, Department of Biotechnology and Nanomedicine, Richard Birkelands vei 3 B, 7034, Trondheim, Norway.

⁴ Área de Bioquímica y Biología Molecular, Departamento de Biología Molecular, Universidad de León, Campus de Vegazana, 24007 León, Spain.

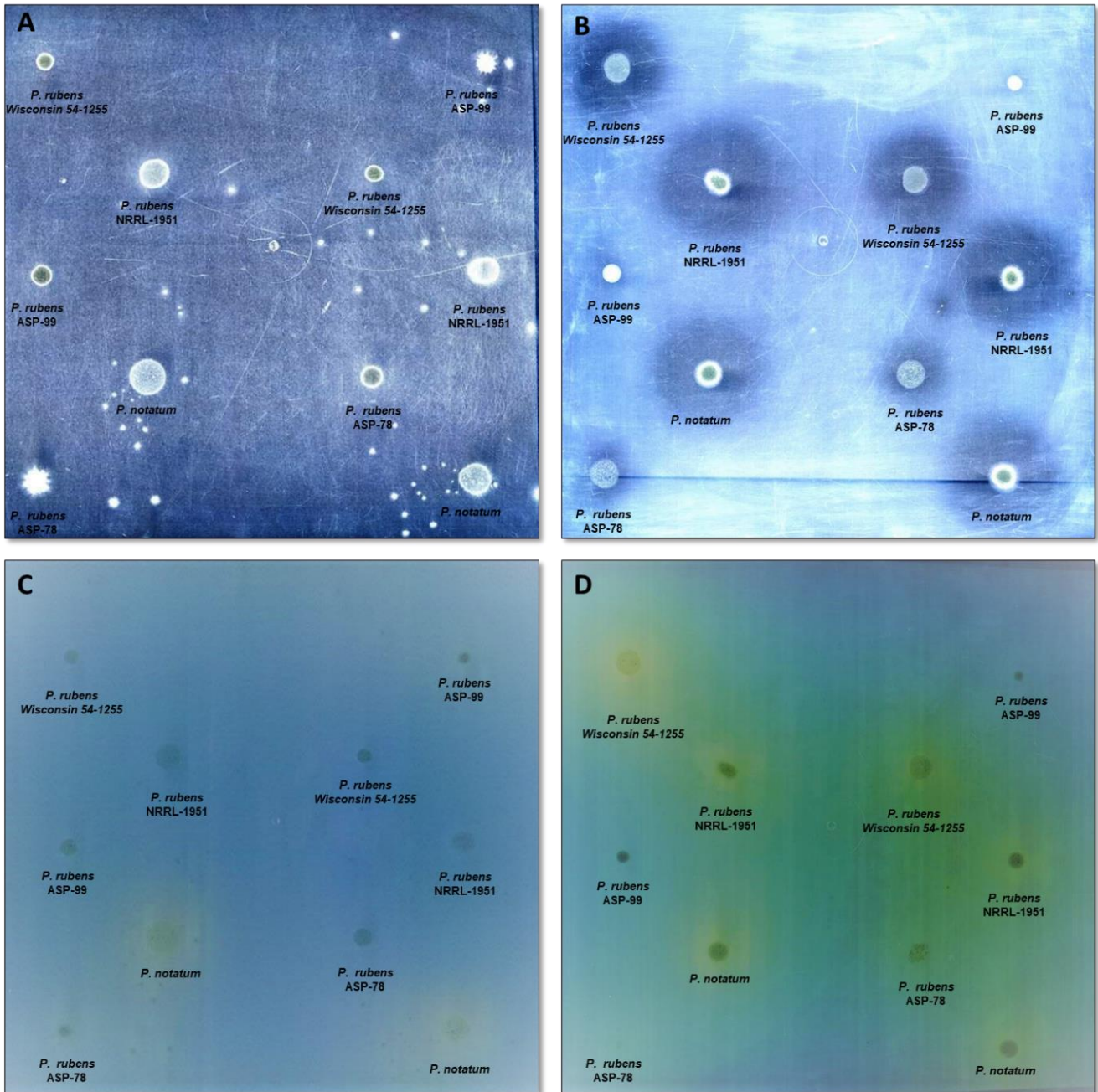
^a Present address: Department of Biotechnology and Food Science; NTNU Norwegian University of Science and Technology, N-7491 Trondheim, Norway.

^b Present address: mAbxience, Upstream Production, Parque Tecnológico de León, Julia Morros, s/n, Armunia, 24009 León, Spain

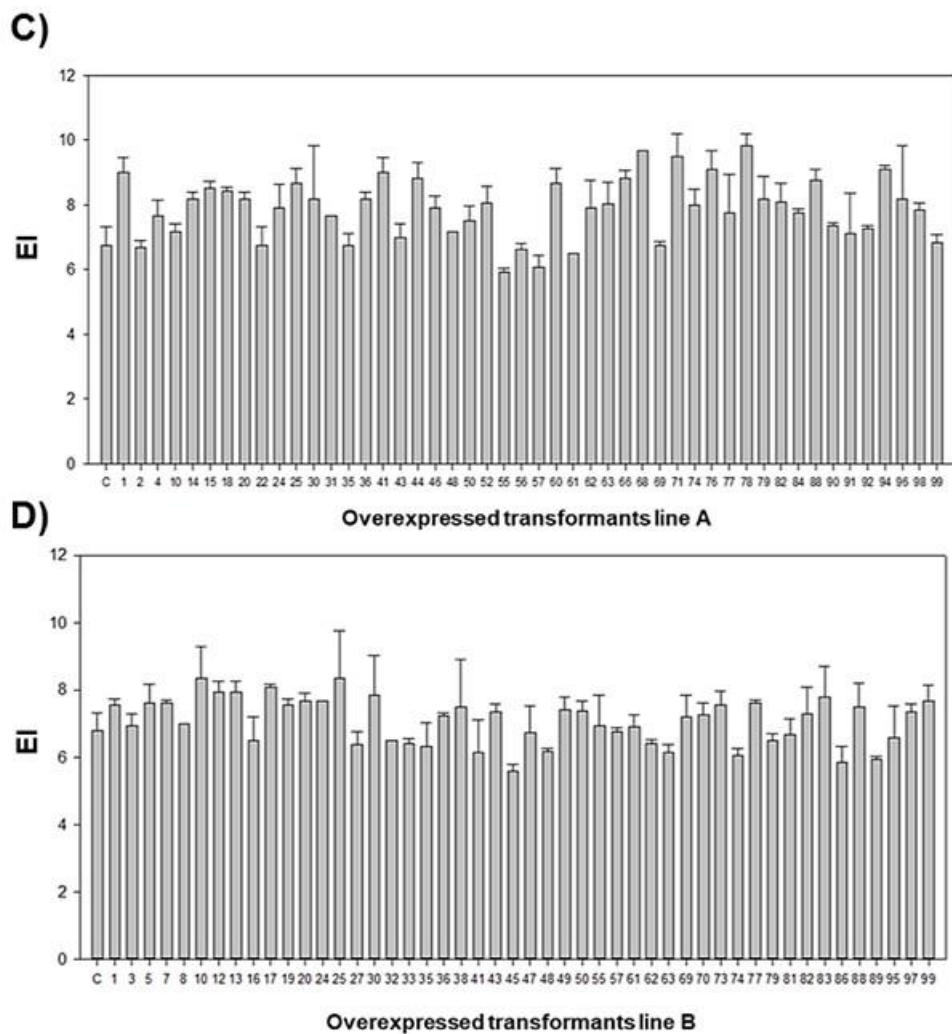
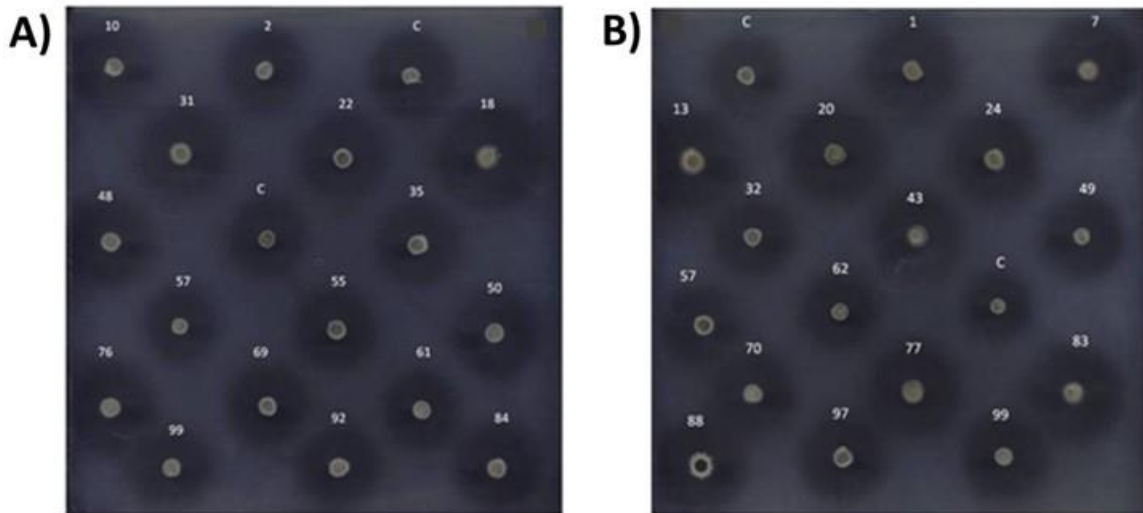
^c Present address: TBI, Université de Toulouse, CNRS, INRAE, INSA, Toulouse 31077, France

§ These authors contributed equally to this work and should be considered co-first authors.

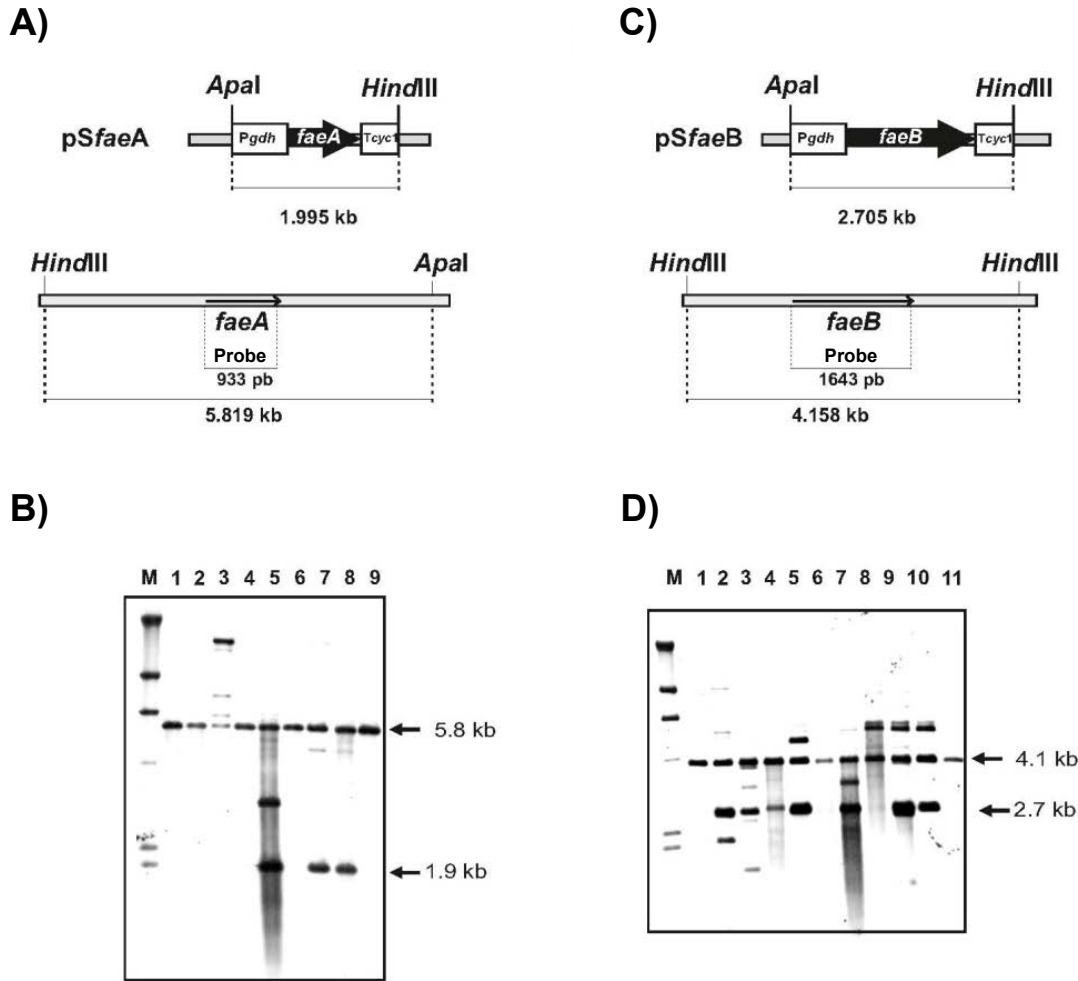
*Corresponding authors: **Dr. Carlos Barreiro** [e-mail: c.barreiro@unileon.es. Phone: +34 987291223. Address: Área de Bioquímica y Biología Molecular, Departamento de Biología Molecular, Universidad de León, Campus de Vegazana, 24007 León, Spain]. **Dr. Ricardo V. Ullán** [e-mail: rvicu@unileon.es. Address: mAbxience, Upstream Production, Parque Tecnológico de León, Julia Morros, s/n, Armunia, 24009 León, Spain].



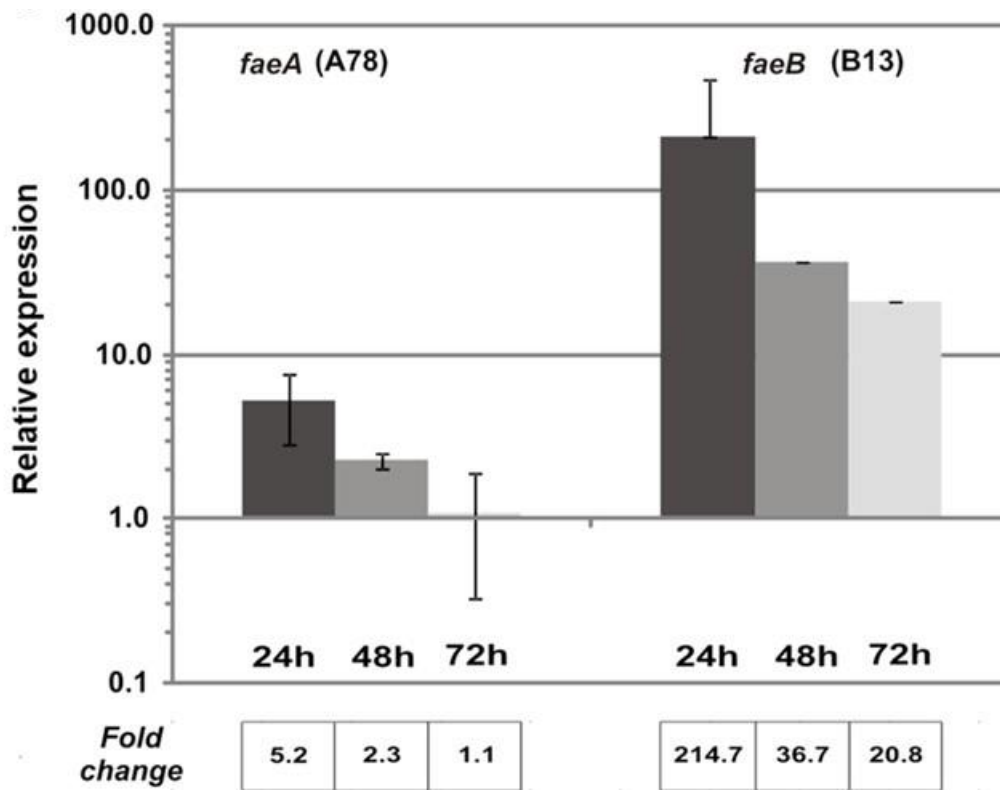
Supplementary Figure S1. FAE activity of several *Penicillium* strains on plate assay. FAE activity is displayed as an EF hydrolysis halo surrounding the colonies. **A)** Control plate without EF. **B)** Plate with EF. **C)** Control plate without EF, stained with bromocresol green. **D)** Plate with EF, stained with bromocresol green.



Supplementary Figure S2. Hydrolysis halos observed in the EF plate assay for some of the 48 transformants chosen from line A (overexpressing *faeA*) (**A**) and from line B (overexpressing *faeB*) (**B**). The parent strain *P. rubens* Wisconsin 54-1255 was used as control (c). **C**) EI of the analyzed transformants from line A. The figure shows averages and standard deviations from three biological replicates. **D**) EI of the analyzed transformants from line B. The figure shows averages and standard deviations from three biological replicates.

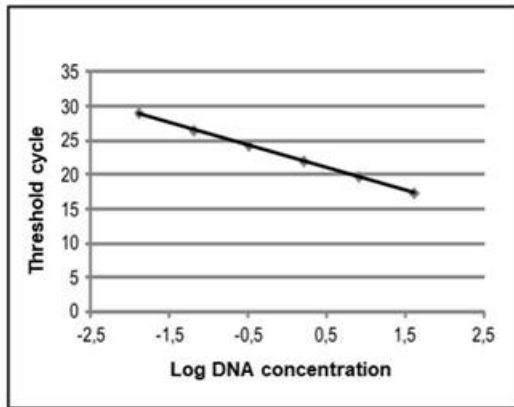


Supplementary Figure S3. Overexpression of *faeA* and *faeB* genes in *P. rubens* Wisconsin 54-1255. **A)** Physical map of the pSfaeA plasmid for the overexpression of *faeA* and schematic representation of the *P. rubens* genome region containing gene *faeA*. The size of the hybridization band of the *Pgdh*-*faeA*-*Tcyc1* expression cassette is indicated. **B)** Southern hybridization of total DNA of 8 transformants and the parent strain *P. rubens* Wisconsin 54-1255 with a 933 bp probe corresponding to the sequence of *faeA*. 1: Wisconsin 54-1255; 2: A1; 3: A18; 4: A31; 5: A68; 6: A71; 7: A76; 8: A78; 9: A84. **C)** Schematic representation of the pSfaeB plasmid, containing the expression cassette *Pgdh*-*faeB*-*Tcyc1*, and the region of the *P. rubens* genome containing *faeB*. **D)** Southern hybridization of total DNA of 10 transformants and the parental strain *P. rubens* Wisconsin 54-1255 with a 1643 bp probe corresponding to the *faeB* gene sequence: 1: Wisconsin 54-1255; 2: B1; 3: B7; 4: B10; 5: B13; 6: B17; 7: B20; 8: B27; 9: B77; 10: B83; 11: B88. M: λ DNA/*HindIII* molecular weight marker labeled with digoxigenin.

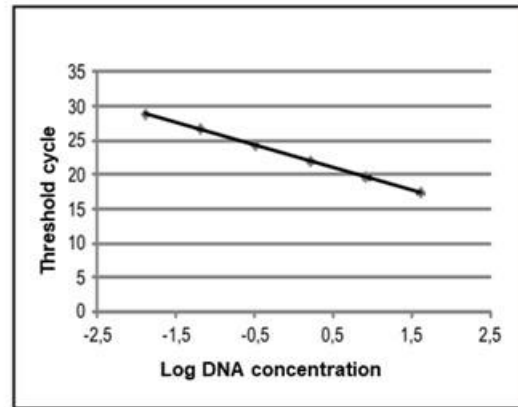


Supplementary Figure S4. Analysis of the expression of *faeA* and *faeB* genes by RT-qPCR in *faeA* overexpressing (A78) and *faeB* overexpressing (B13) *P. rubens* transformants. Relative values refer to the expression values for each *fae* gene in the parent strain *P. rubens* Wisconsin 54-1255. The expression of *actA* (encoding Y-actin) was used as a control. Error bars indicate the standard deviation of the ratio value between three biological replicates and three technical replicates of each sample. Fold change values are shown.

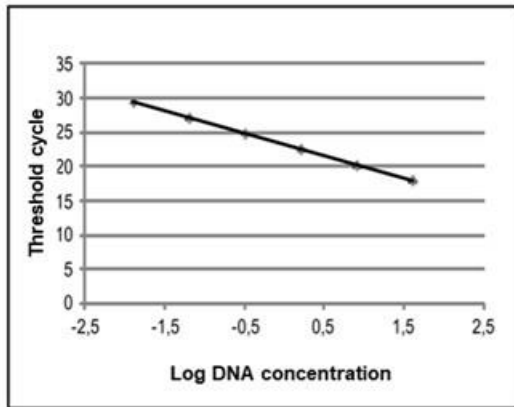
A) *faeA*



B) *faeB*



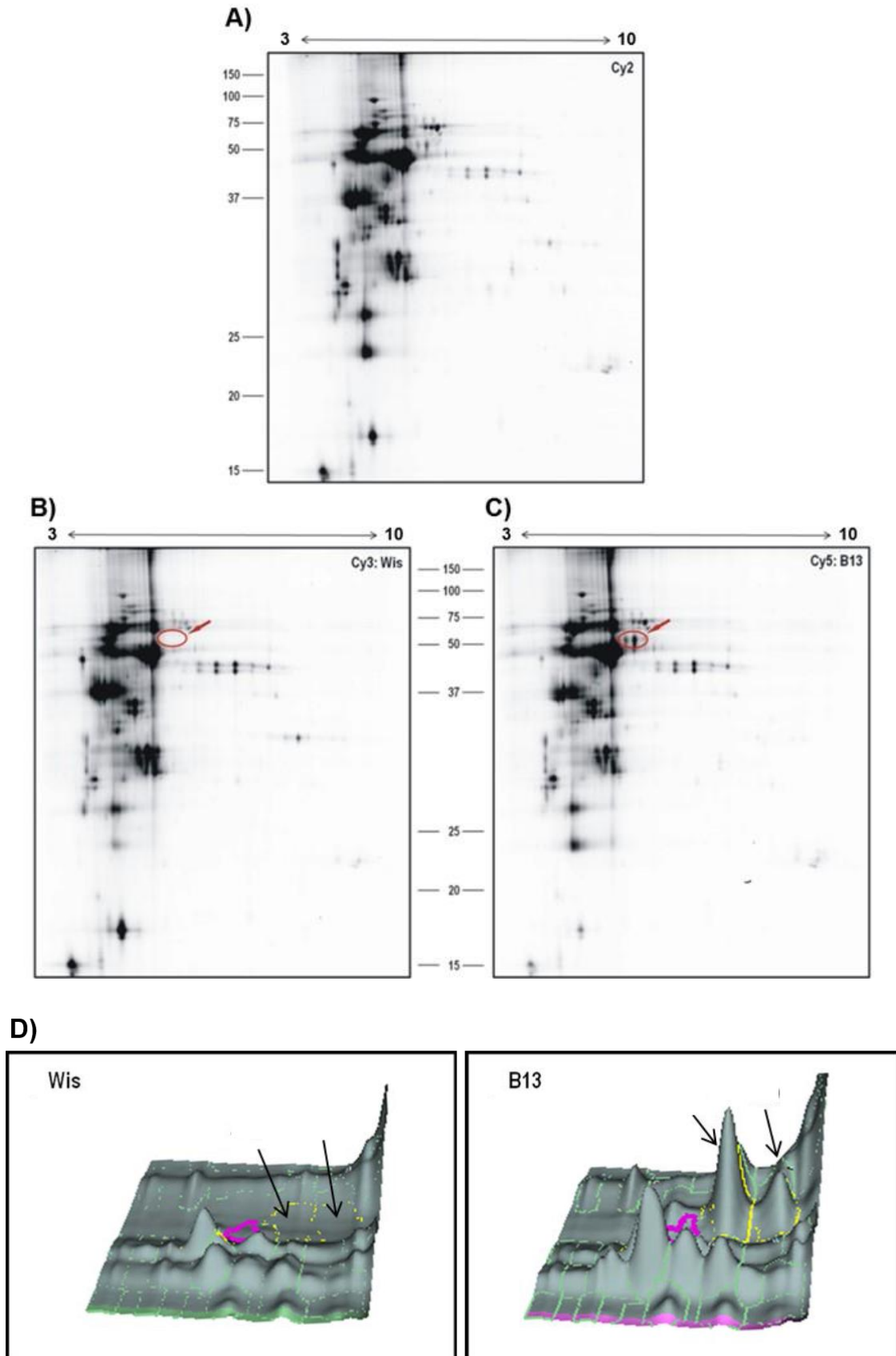
C) *act*



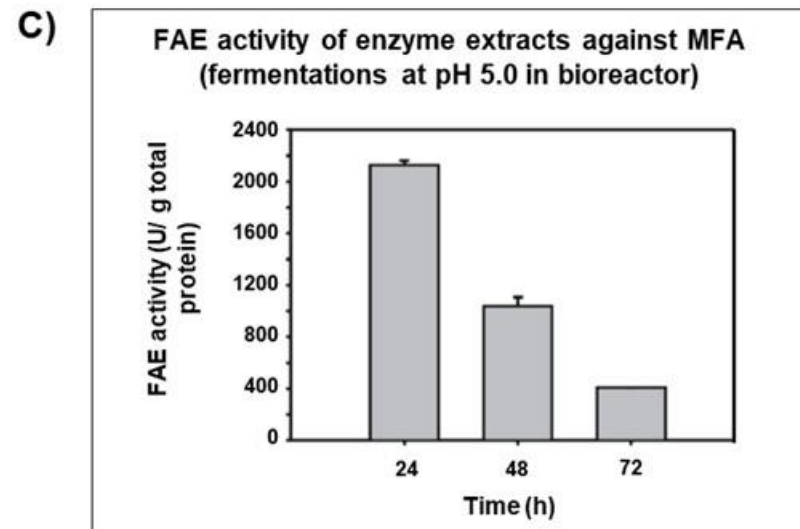
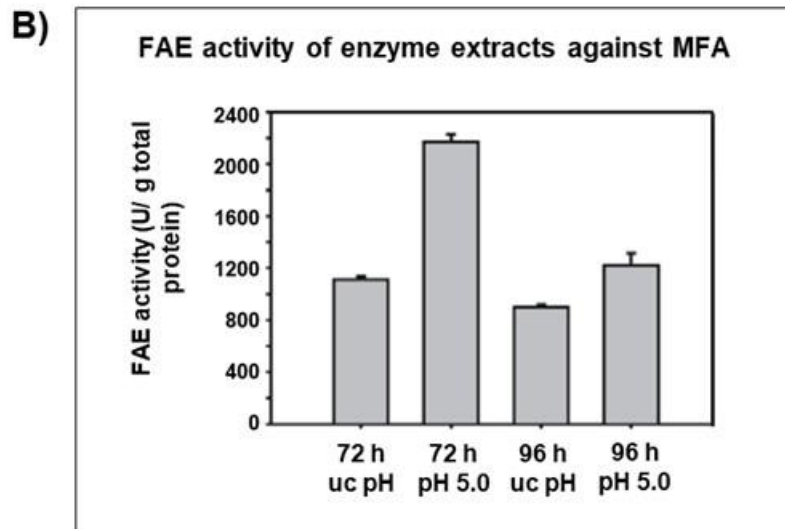
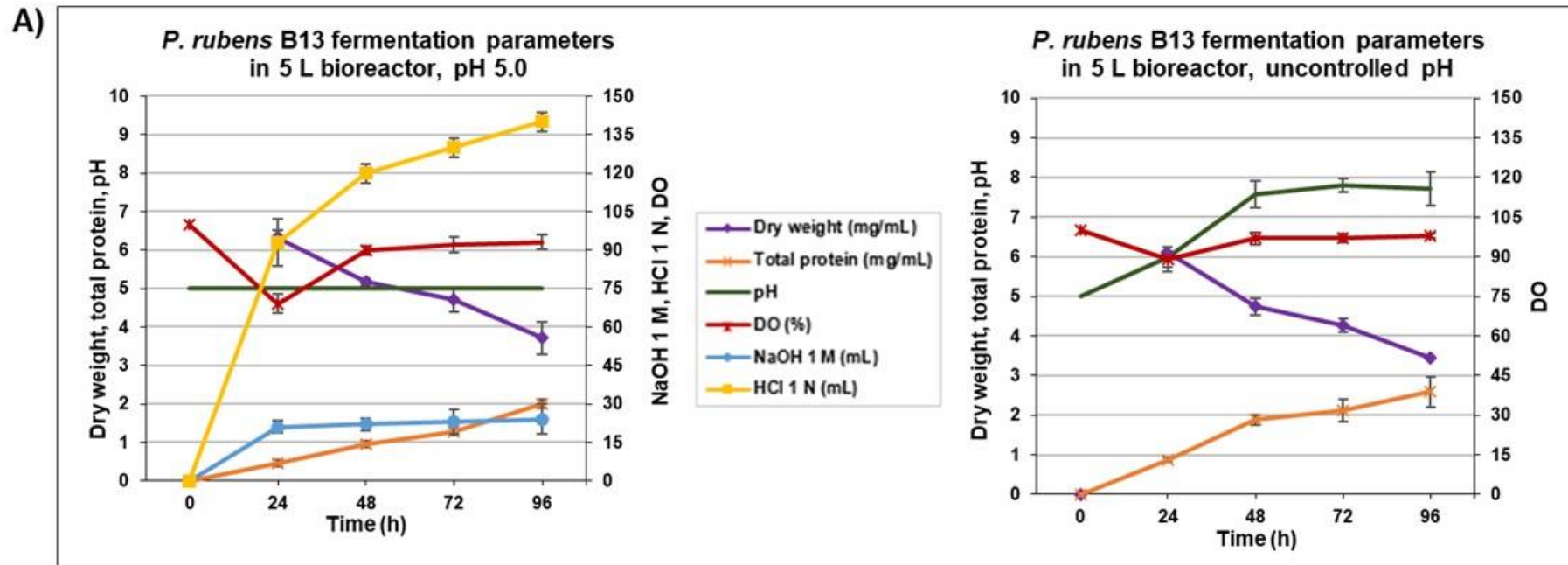
D)

	Slope	R^2	Efficiency
L <i>faeA</i> /R <i>faeA</i>	-3.3104	0.999	1.00
L <i>faeB</i> /R <i>faeB</i>	-3.2856	0.999	1.01
L <i>act</i> /R <i>act</i>	-3.2855	0.999	1.01

Supplementary Figure S5. Efficiency of the RT-qPCR amplification. Representation of the standard concentrations of DNA vs. the threshold cycle, to calculate the efficiency of amplification for the different analyzed genes: *faeA* (A), *faeB* (B), and *actA* (C). D) Slope, R^2 , and efficiency of the amplification data for each of the amplified cDNA fragments of the analyzed genes.

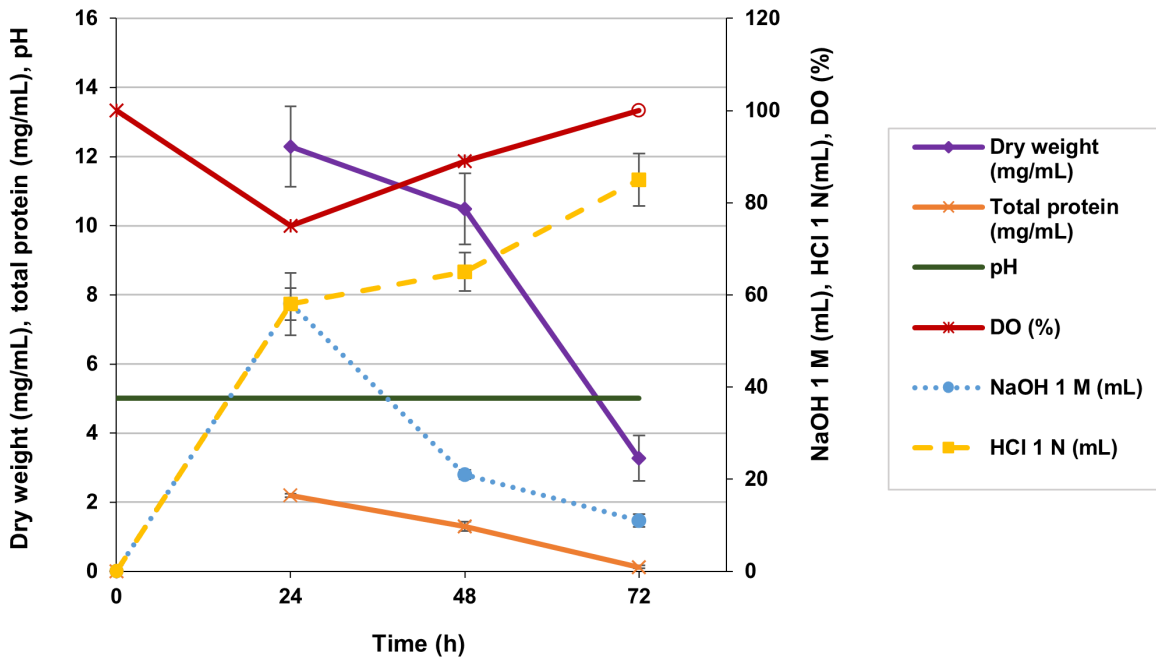


Supplementary Figure S6. 2D-DIGE analysis of differences in the extracellular protein production by *P. rubens* Wisconsin 54-1255 (Wis) and B13 strains, grown on M-SBP medium for FAE production. A) Internal standard (Cy2). B) *P. rubens* Wisconsin 54-1255 strain (Cy3). C) *P. rubens* B13 strain (Cy5). D) 3D representation on DeCyder software (GE Healthcare) of the abundance of the two protein spots identified as PrFaeB (Pc12g08300) in both strains. Arrows indicate the two protein spots identified as PrFaeB.

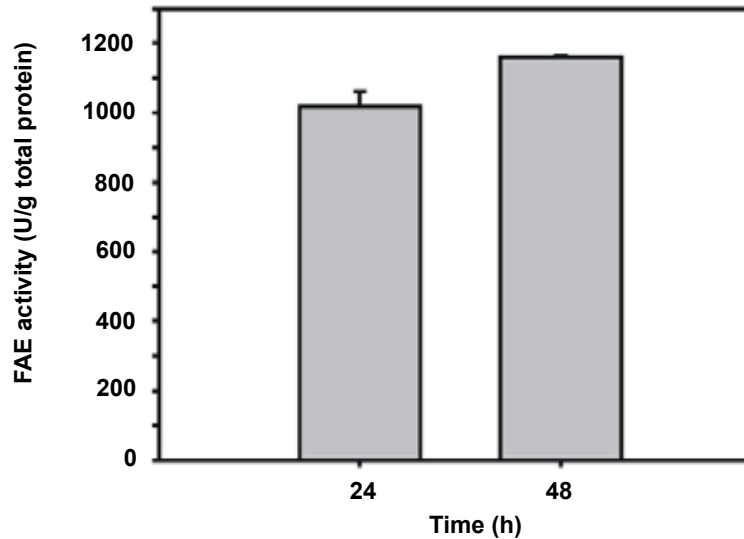


Supplementary Figure S8. Fermentation parameters and FAE activity of *P. rubens* B13 in 5 L bioreactors with M-SBP medium [U= unit; amount of enzyme that releases one μmol of ferulic acid per min under the tested conditions (20 min reactions at pH 5.0 and 50 °C)]. **A)** Fermentation parameters in 5 L bioreactors at pH 5.0 (left) and uncontrolled pH (right). **B)** FAE activity against MFA of enzyme extracts recovered at 72 and 96 h from fermentations in a bioreactor carried out at 28 °C, at pH 5.0 and uncontrolled pH (uc pH). **C)** FAE activity against MFA of enzyme extracts recovered at 24, 48, and 72 h from fermentations in a bioreactor carried out at 28 °C and pH 5.0.

A) *P. rubens* B13 fermentation parameters in 20 L bioreactor, pH 5.0



B) FAE activity of enzyme extracts against MFA (20 L bioreactor)



Supplementary Figure S9. Fermentation parameters and FAE activity of *P. rubens* B13 in 20 L bioreactors with M-SBP medium. **A)** Fermentation parameters in 20 L bioreactors at 28 °C and pH 5.0. The figure shows values for dry weight (mg/mL), total protein (mg/mL), pH, DO (%), NaOH 1 M (mL added since the previous time-point), HCl 1 M (mL added since previous time-point) **B)** FAE activity against MFA of enzyme extracts recovered at 24 and 48 h from fermentations in 20 L bioreactors, containing M-SBP medium, at 28 °C and pH 5.0. FAE activity is expressed in U/g protein from enzyme extract [U= unit; amount of enzyme that releases one μmol of ferulic acid per min under the tested conditions (20 min reactions at pH 5.0 and 50 °C)].